琉球大学学術リポジトリ

ウォレスの古代湖での同所的種分化

メタデータ	言語: English 出版者: 琉球大学 公開日: 2021-10-04 キーワード (Ja): キーワード (En): 作成者: Nobu, Sutra メールアドレス: 所属:
URL	http://hdl.handle.net/20.500.12000/49806

Doctoral Thesis of Philosophy

Sympatric speciation in a Wallacean ancient lake

September 2021

by

SUTRA NOBU

Marine Biology
Marine and Environmental Sciences
Graduate School of Engineering and Sciences
University of the Ryukyus

Supervisor: Prof. Kazunori Yamahira

Thesis/Dissertation Title:
Sympatric speciation in a Wallacean ancient lake

Name: Sutra Nobu

We, the undersigned, hereby, declare that we have read this thesis and we have attended the thesis defense and evaluation meeting. Therefore, we certify that, to the best of our knowledge this thesis is satisfactory to the scope and quality as a thesis for the degree of Doctor of Philosophy in Marine Biology under Major Marine and Environmental Sciences, Graduate School of Engineering and Science, University of the Ryukyus.

THESIS/DISSERTATION REVIEW & EVALUATION COMMITTEE MEMBERS

Signature

(Chairman) Kazunori Yamahira

Signature

(Committee) Mamoru Toda

Signature

(Committee) James D. Reimer

Signature

(Committee) Ryosuke Kimura

Author's Publication List

Sutra, N., Kusumi, J., Montenegro, J., Kobayashi, H., Fujimoto, S., Masengi, K. W. A., Nagano, A.J., Toyoda, A., Matsunami, M., Kimura, R., and Yamahira, K. (2019). Evidence for sympatric speciation in a Wallacean ancient lake. *Evolution*, 73, 1898-1915, doi:10.1111/evo.13821

Kakioka, R*., Sutra, N*., Kobayashi, H., Ansai, S., Masengi, K. W. A., Nagano, A.J.,Okuda, N., Tanaka, R., Sato, M., and Yamahira, K. (2021). Resource partitioning is not coupled with assortative mating of in sympatrically divergent ricefish in a Wallacean ancient lake. *Journal of Evolutionary Biology*, JEB13874, doi: 10.1111/jeb.13874

*equally contributed

Acknowlegedments

All the praises to the Almighty ALLAH SWT who has been blessing me with uncountable graces. Who granted me precious opportunities for pursuing my doctoral degree and always granting me with so much love, loading me with full of will and determination thus could accomplish this academic pathway.

I would like to express my sincere gratitude and respect to my supervisor Professor Yamahira Kazunori, Tropical Biosphere Research Center, University of the Ryukyus, for giving me the opportunity to become his student and giving me a chance to study sympatric speciation in a Wallacean ancient lake, guiding me to grow better as a researcher, and keeping on believing in me throughout the process until I could finally accomplish my doctoral degree.

I would also like to thank Professor James D. Reimer, Department of Chemistry, Biology, and Marine Science, University of the Ryukyus, Professor Mamoru Toda, Tropical Biosphere Research Center, University of the Ryukyus, and Professor Ryosuke Kimura, Department of Human Biology and Anatomy, Graduate School of Medicine, University of the Ryukyus for their moral assistance, guidance and constant encouragement.

I thank my close friends and colleagues from Tropical Biosphere Research Center (TBRC) office and Laboratory group. Special thank to Ryo Kakioka, Ixchel Fiebe Mandagi, Javier Montenegro, Hirozumi Kobayashi, Daniel Frikli Mokodongan, Bayu K Aditya, Teppei Jono and TBRC's laboratory members for their helps with analysis, advice and guidance.

I would like thank to the Ministry of Education, Culture, Sports, Science, and Technology (MEXT) of Japan for the Japanese government (Monbusho) scholarship for opening opportunities and providing the financial supports through Coral Reef and Advanced Biology Science (CRABS) program, University of the Ryukyus during my study.

I would like to thank the Ministry of Research, Technology and Higher Education of Republic of Indonesia, Faculty of Fisheries and Marine Science, Sam Ratulangi University and Faculty of Marine Science and Fisheries, Hasanuddin University, for the permits to conduct research in Sulawesi, Indonesia.

Finally, I would like to express my love and gratitude to my parents Sutriani Manangkasi and Shigenobu Fujioka for all the love supports and the prayers, to my husband Joseph Ryan Limoli who always been my number one supporter in every step I had made. To my beloved daughters Asqirah Aprilia Limoli and Arsyifa Keiko Okinawa Limoli for bringing so much bless and happiness to my life. To my sister Shigerani Natalia, my brother

in-law Dr. Fauzi R. Rahim, my brother Nur Resky and also my big families for always supporting me in so many ways. To the big family of Persatuan Pelajar Indonesia di Okinawa (PPOI) for all the solidarity and caring.

Table of contents

Contents **Page**

Abstract iii
Author's Publication List v
Acknowledgements vi
Table of Contents viii
List of Figures x
List of Tables xiv

Chapter 1
General introduction 1

Chapter 2
Evidence for sympatric speciation 4
2.1 Introduction 4
2.2 Material and Methods 5
2.2.1 Field Collection 5
2.2.2 Morphological Analyses 6
2.2.3 Mitochondrial DNA Sequencing 7
2.2.4 ddRAD Sequencing 7
2.2.5 Phylogenetic Analysis 11
2.2.6 Population-Structure Analysis 12
2.2.7 Divergence-Time Estimation 12
2.3 Results 13
2.3.1 Morphology 13
2.3.2 Phylogeny 14
2.3.3 Population Structure 14
2.3.4 Divergence Time 15
2.4 Discussion 15
2.4.1 Monophyly and Reproductive Isolation of Sympatric Species 15
2.4.2 No Historical Phase of Geographic Isolation During Speciation 17
2.4.3 A New case example of sympatric speciation 17

Chapter 3

Resource partitioning and assortative mating 19
3.1 Introduction 19
3.2 Material and Methods 20
3.2.1 Field Collections and Underwater Observations 20
3.2.2 Population structural analyses 21
3.2.3 Morphological analyses 22
3.2.4 Stable Isotope Analyses 23
3.2.5 Measurements of Eggs Characteristics 23
3.2.6 Mating Experiments 24
3.2.7 Statistical Analyses 25
3.3 Results 26
3.3.1 Intra-lake population structure 26
3.3.2 Morphologies 26
3.3.3 Feeding behaviors and stable isotope analyses 27
3.3.4 Spawning sites and egg characteristics 28
3.3.5 Mating behaviors of *O. nebulosus* and *O. orthognathus* 28
3.4 Discussion 30
3.4.1 Resource partitioning among *Oryzias* in Lake Poso 30
3.4.2 Assortative mating *Oryzias* in Lake Poso 31
3.4.3 Sympatric speciation without magic? 32

Chapter 4

General discussion 34
4.1 How has sympatric speciation been completed without magic traits 34
4.2 A new model system for the study on sympatric speciation 36

References 38

Figures

Figure **Page**

Figure 1. Schematic illustration of the process of (A) allopatric speciation and (B) sympatric speciation 65

Figure 2. Schematic illustration of the four criteria by Coyne and Orr (2004) necessary to be satisfied to demonstrate sympatric speciation, i.e., (A) sympatric contemporary distributions, (B) genetically-based reproductive isolation, (C) phylogenetic sister relationships, and (D) no historic phase of geographic isolation. 66

Figure 3. Schematic illustration to explain why resource partitioning must be coupled assortative mating for sympatric speciation to be completed. (A) If resource partitioning (shown as large vs. small mouths) and assortative mating (shown as red vs. blue colors) are coupled in some ways, i.e., if individuals with large (small) mouths are always blue (red), sympatric speciation will be completed. "Automatic magic traits", which allow populations not only to use different resources but also to mate assortatively as a byproduct of resource partitioning, would generate this situation. (B) If resource partitioning and assortative mating are not coupled, i.e., if some individuals with large (small) mouths are red (blue), sympatric speciation will not be completed, because individuals having different resource utilization will mate with each other. 67

Figure 4. Maximum likelihood (ML) phylogeny of Sulawesi adrianichthyids based on mtDNA sequences (ND2: 1,053 bp; cyt *b*: 1,141 bp) and a map showing locations of the collection sites. The water systems of Lake Poso and Lake Tiu are indicated by blue and red, respectively. Map provided by Thomas von Rintelen and modified. See Supplementary Methods and Results and Table S1 for how to estimate the ML tree 68

Figure 5. Bathymetry map of Lake Poso, showing locations of sites where riverine *Oryzias* were searched for. Map modified from Rintelen et al. (2012), with permission 69

Figure 6. (A) Relationships between the standard length and body depth of the three sympatric *Oryzias* species. (B) Scatterplot of the first two axes of the principal component analysis based on the meristic characters. Circles and triangles represent fish collected from Lake Poso at Saluopa and Dumulanga, respectively 70

Figure 7. Maximum-likelihood and neighbor-joining phylogenies of the three Poso *Oryzias* species with their outgroup, based on (A) the 2,194-bp concatenated mitochondrial sequences and (B) the 157,029-bp concatenated RAD sequences, respectively. Numbers on branches are bootstrap values 71
Figure 8. Neighbor-net phylogenetic networks based on Nei's genetic distances calculated from the 2,718 SNPs. Circles and triangles represent individuals collected from Saluopa and Dumulanga, respectively. 72
Figure 9. Species tree for the four *Oryzias* species estimated by SNAPP, based on 2,718 SNPs. Thin lines represent individual speciation trees 73
Figure 10. Cross-validation errors for the ADMIXTURE runs 74
Figure 11. Results of ADMIXTURE analyses showing K = 2–5 genetic clusters, based on the 2,718 SNPs 75
Figure 12. Principal components analysis of genetic variance among the four *Oryzias* species based on the 2,718 SNP dataset 76
Figure 13. Bayesian chronogram based on the mtDNA sequences (ND2: 1,053 bp; cyt b: 1,141 bp), using substitution rates of 2.80% and 2.65% per Myr for ND2 and cyt b, respectively. Numbers on branches are Bayesian posterior probabilities. Bars represent 95% high posterior density 77
Figure 14. Visualization of possible introgression based on the 2,718 SNPs. (A) Maximum-likelihood trees, fitting (A) no migration (m = 0) and (B) one migration event (m = 1). The direction of gene flow is indicated by an arrow, and heat colors reflect intensity. Heat maps indicate the residual covariance among species pairs given the respective trees assuming that (C) m = 0 and (D) m = 1. Note that no covariance remained when m = 1 78
Figure 15. A map showing locations of the collection sites and species trees of three *Oryzias* species in Lake Poso. The map was provided by Thomas von Rintelen and modified. Species trees were modified after Sutra et al. (2019) 79
Figure 16. Cross-validation errors for the ADMIXTURE runs 80
Figure 17. ADMIXTURE results showing K = 2–4 genetic clusters based on the 0,000 SNPs among four populations 81
Figure 18. Principle component analysis of genetic variance among the three Oryzias species based on the 0,000 SNP dataset 82
Figure 19. Scatterplot of the first two axes of principal component analyses based on the geometric morphometric dataset and deformation grids showing the

maximum shape changes along each axis. Diamonds and circles represent males and females, respectively 83
Figure 20. Relationship between the standard length and digestive tract length of the three Oryzias species. Diamonds and circles represent males and females, respectively 84
Figure 21. Relationship between the standard length and gill arch length of the three Oryzias species. Diamonds and circles represent males and females, respectively. The interspecific difference in gill arch length was significant after correcting the body size (ANCOVA, $F_{2,59} = 60.9493$, $P < 0.0001$). The difference was significant (Turkey's HSD tests, $P < 0.05$) in all species pairs 85
Figure 22. Length and distribution of each gill raker of the three *Oryzias* species 86
Figure 23. Pictures of fresh digestive tracts of the three Oryzias species 87
Figure 24. Plots of δ13C versus δ15N values of the three Oryzias species. Diamonds and circles represent males and females, respectively 88
Figure 25. The spawning site of Oryzias nebulosus and O. orthognathus at Dumulanga. Darker and paler individuals are O. nebulosus and O. orthognathus, respectively 89
Figure 26. Egg diameters of the three Oryzias species. The line, box and whisker represent median, (upper and lower) quartiles, and range, respectively 90
Figure 27. Time until spawning by each female of Oryzias nebulosus and O. orthognathus. Each line represents the average time (± SD) of one individual female mated with a male from the same versus different species 91
Figure 28. Summary of (A) resource partitioning and (B) assortative mating among the three Poso *Oryzias* species. Note that the difference in feeding sites between *O. nigrimas* and *O. nebulosus* may be an "automatic magic trait" leading to a "mate-where-you-eat" preference. However, no such automatic magic trait is evident between *O. nigrimas* and *O. orthognathus* or between *O. nebulosus*, and *O. orthognathus*. 92
Figure 29. Schematic illustration to explain how sympatric speciation can be completed even without automatic magic traits. (A) Sympatric speciation with an automatic magic trait; sympatric speciation is considered to be completed, if resource partitioning and assortative mating are automatically coupled with each other. In contrast, (B) sympatric speciation would be possible even without such automatic magic traits, if there is a strong postzygotic isolation between

diverging populations. The low-productivity ecosystem in Lake Poso would generate this situation, because hybrid individuals might not exploit the food resources.

Tables

Table **Page**

Table 1. Substitution models used in the BEAST analyses 51

Table 2. Results of ANOVA of the effects of standard length, species, sex, and their interactions on body depth 52

Table 3. Frequency distributions for (A) the number of scales along the lateral midline, (B) the number of pectoral-fin rays, (C) the number of anal-fin rays, and (D) the number of vertebrae, for the three Oryzias species endemic to Lake Poso. Numbers in parentheses indicate the number of males 53

Table 4. Results of ANOVA of the effects of species, sex, and their interaction on (A) PC1 and (B) PC2 54

Table 5. List of samples used in this study. PSA, MA, and SIA represent population structure analyses, morphological analyses, and stable isotope analyses 55

Table 6. Results of two-way analyses of variance of the effects of species and sex on (a) PC1 and (b) PC2 scores in the geometric morphometric analysis 56

Table 7. Result of two-way analysis of covariance of the effects of standard length, species, and sex on digestive tract length 57

Table 8. Result of two-way analysis of covariance of the effects of standard length, species, and sex on gill arch length 58

Table 9. Result of two-way analysis of variance of the effects of species and sex on gill raker number 59

Table 10. Results of two-way analyses of variance of the effects of species and sex on (a) gill raker length and (b) gill raker interval 60

Table 11. Results of two-way analysis of variance of the effects of species and sex on (a) $\delta^{13}C$ and (b) $\delta^{15}N$ values in the stable isotope analyses 61

Table 12. Result of partially nested three-way analysis of variance of the effects of male species (conspecific versus heterospecific), female species, and female individual (nested within female species) on average time until spawning 62

Table 13. Day of first spawning in each of the intra- and interspecific mating trials. Numbers indicate the frequency of days upon which the first spawning occurred

among the nine combinations of pairs (i.e., round robin among three females and three males) 63

Table 14. Color change sequences involved in mating behaviors. Numbers indicate frequency of each sequence among 27 observations of mating behaviors (i.e., three replicates of each of the nine combinations of pairs). MB: male became black; FB: female became black; and MW: male became whitish. Note that all females that became black spawned thereafter 64

ABSTRACT

Sympatric speciation, the process through which new species evolve from a single ancestral species in the absence of geographical barriers, has been a central subject in evolutionary biology since Darwin's "principle of divergence". Sympatric speciation is considered to be difficult, because automatic magic traits, i.e., the coupling between ecological traits that allow resource partitioning and reproductive traits that allow assortative mating, are necessary for it to complete. Indeed, only a few empirical case studies demonstrating this mode of speciation are known. Some consider that this is due not to its rarity, but because of the difficulty of empirically demonstrating this mode of speciation. In this study, I examined a possible case of sympatric speciation in three ricefish species of the genus *Oryzias*, *O. nigrimas*, *O. nebulosus* and *O. orthognathus*, which are endemic to Lake Poso, an ancient tectonic lake in central Sulawesi.

First, I tested if the three *Oryzias* species satisfy all criteria necessary to demonstrate sympatric speciation. Phylogenetic analyses using RAD-seq-derived single nucleotide polymorphisms (SNPs) revealed that the three *Oryzias* species are monophyletic. I also found that the three species are morphologically distinguishable and clearly separated by population-structure analyses based on the SNPs, suggesting that they are reproductively isolated from each other. A mitochondrial DNA chronogram suggested that their speciation events occurred after the formation of the tectonic lake, and the existence of a historical allopatric phase was not supported by coalescent-based demographic inference. These results all concur with the criteria for sympatric speciation.

Second, I examined resource partitioning and assortative mating in the three species. Stable isotope analyses revealed that the three species use different food resources, which reflect differences in their feeding morphologies (gill rakers and digestive tracts) and feeding

sites. Field and laboratory observations showed that *O. nebulosus* and *O. orthognathus* share a mating habitat of cobbles, where they scatter fertilized eggs, whereas this site is never used by *O. nigrimas*, indicating that assortative mating is partly achieved by spatial isolation. The small, less-adhesive eggs of *O. nebulosus* and *O. orthognathus* probably reflect their adaptation to spawning on cobble beaches. Laboratory mating experiments showed strong prezygotic isolation between *O. nebulosus* and *O. orthognathus*, which is achieved by strong species recognition presumably by both sexes based on species-specific mating dances and nuptial coloration. Thus, the assortative mating of *O. nebulosus* and *O. orthognathus* was probably not coupled to resource partitioning.

In summary, it is highly probable that the three *Oryzias* species in Lake Poso have diverged in sympatry, but that, contrary to theories, the sympatric divergences have been completed without automatic magic traits. This is especially true for the divergence between *O. nebulosus* and *O. orthognathus*. The ricefishes in this Wallacean lake provide a promising new model system for the study of sympatric speciation.

CHAPTER 1

GENERAL INTRODUCTION

The origin of species has been one of the most controversial topics in biology (Bolnick and Fitzpatrick 2007). Speciation, or the process through which new species arise, has been considered essential evens in the history of life. In speciation, an ancestral species splits into descendant species that can no longer interbreed. Allopatric speciation, in which new species arise as a result of geographic isolation (Fig. 1A), is an uncontroversial theory with numerous observed and experimental examples (Coyne and Orr 2004). In contrast, sympatric speciation, through which new species evolve in the absence of geographical barriers (Fig. 1B), has been a central subject in evolutionary biology since Darwin's "principle of divergence" (e.g., Mayr 1992; Turelli et al. 2001). Although subsequent theories contend that sympatric speciation is possible under certain conditions (e.g., Dieckmann and Doebeli 1999; Higashi et al. 1999; Kondrashov and Kondrashov 1999; see Bolnick and Fitzpatrick 2007 for review), only a few empirical case studies demonstrating this mode of speciation are known (see below and Bolnick and Fitzpatrick 2007 for review).

Sympatric speciation has been reported both from animals and plants. African cichlid fishes offer well-known examples of sympatric speciation, in which species pairs have adapted to different depths within single lakes (e.g., Schliewen et al. 1994; Seehausen et al. 2008). Host races of North American fruit flies of the genus *Rhagoletis* are also an example of ongoing speciation in sympatry. One selectively oviposits on fruits of a native plant species, whereas the other is shifting to domesticated apples, leading to spatial and temporal reproductive isolation between the incipient fly species. (Feder and Bush 1989). Southwest African indigobirds *Vidua* spp., which are host-specific brood parasites, have speciated sympatrically by switching to new host bird species that have colonized recently (Sorenson et

al. 2003). Sympatric speciation of *Howea* palm trees on Lord Howe Island, east off Australia, has been achieved by the differentiation in soil usage and the timing of flowering after their common ancestor colonized the oceanic island (Savolainen et al. 2006).

It is proposed that four criteria need to be satisfied to demonstrate sympatric speciation (Coyne and Orr 2004): (i) sympatric contemporary distributions (i.e., the species must be largely or completely sympatric), (ii) substantial reproductive isolation (i.e., the sympatric species do not interbreed), (iii) phylogenetic sister relationships (i.e., the sympatric species are each other's closest relatives), and (iv) no historical phase of geographic isolation (i.e., the existence of an allopatric phase during divergence is very unlikely) (Fig. 2). However, these criteria are often difficult to be tested. For example, a small number of genetic markers might not be sufficient to capture the establishment of reproductive isolation (criterion ii) when genetic difference between the species is slight (e.g., Kutschera et al. 2014; Zhou et al. 2017; Marques et al. 2019). Similarly, inferences of the phylogenetic sister relationship (criterion iii) may be misguided when only data for mitochondrial DNA (mtDNA) and/or a small number of nuclear genes are used (Maddison 1997; Nichols 2001). The absence of an allopatric phase in the past (criterion iv) is also generally difficult to demonstrate because it requires concrete knowledge of the geological history of the relevant region and the biogeographic history of the species themselves. Therefore, very few case studies have met these criteria despite intensive searches (Coyne and Orr 2004; Bolnick and Fitzpatrick 2007).

In contrast, sympatric speciation may be actually rare. Theories predict that sympatric speciation generally requires both resource partitioning by disruptive selection and assortative mating by mate preference and/or spatial or temporal reproductive isolation (Fig. 3A) (Felsenstein 1981; Dieckmann and Doebeli 1999; Kondrashov and Kondrashov 1999; Doebeli et al. 2005). The major obstacle to sympatric speciation is that recombination would erode the coupling between the ecological traits that allow resource partitioning and the

reproductive traits that enable assortative mating (Fig. 3B) (Dieckmann and Doebeli 1999; Kondrashov and Kondrashov 1999; Doebeli et al. 2005; Kopp et al. 2018). Therefore, if ecological traits and reproductive traits are combined in some way, sympatric speciation would be much easier. Such “magic traits” are known to be involved in most of the compelling examples of sympatric speciation (Via 1999; Berlocher and Feder 2002; Forbes et al. 2009; Hadid et al. 2013). In particular, “automatic magic traits”, which allow populations not only to use different resources but also to mate assortatively as a byproduct of resource partitioning (Servedio et al. 2011), are proposed to be a requirement for the completion of sympatric speciation (Martin 2013; Martin et al. 2015).

Three species of ricefishes of the genus *Oryzia*s, namely *O. nebulosus* Parenti and Soeroto, *O. orthognathus* Kottelat, and *O. nigrimas* Kottelat, are known to be endemic to Lake Poso, an ancient tectonic lake on Sulawesi Island (Kottelat 1990; Parenti and Soeroto 2004). The mtDNA phylogenies suggested that these three species are monophyletic (Fig. 4) (Mokodongan and Yamahira 2015a, b). In this study, I first test the four criteria by Coyne and Orr (2004), using morphologies and population-genomic analysis of genome-wide single-nucleotide polymorphisms (SNPs), and demonstrate that these three *Oryzias* species have diverged within the lake in sympatry. Second, I investigate resource partitioning and assortative mating of the three species and demonstrate that this sympatric speciation was completed with no automatic magic trait, and probably with no magic trait of any other form. Based on these findings, I finally discuss how the sympatric speciation in this ancient lake could be completed even without magic traits.

CHAPTER 2

EVIDENCE OF SYMPATRIC SPECIATION

2.1 INTRODUCTION

Sulawesi is the largest island of Wallacea, a group of islands located between the Sunda Shelf and the continental shelf of Australia. Previous molecular phylogenetic analyses revealed that these Sulawesi adrianichtyids are monophyletic (Takehana et al. 2005; Herder et al. 2012; Mokodongan and Yamahira 2015a, b; Mandagi et al. 2018), suggesting that they diverged within the island from a single common ancestor. It has been demonstrated that the divergence of major clades from this common ancestor largely reflects the complex geological history of this island (Mokodongan and Yamahira 2015a). Especially, most species in the late-branching lineages are endemic to a single tectonic lake or lake system in central Sulawesi, suggesting that habitat fragmentation due to the final collision/juxtaposition processes of tectonic subdivisions in this island since the Pliocene and the resultant lake formations are the primary factors promoting diversification of these lacustrine lineages and shape their current distributions (Fig. 4) (Mokodongan and Yamahira 2015a). However, it remains unclear in most cases how species within each lineage have diverged.

Three species of *Oryzia*s, *O. nebulosus* Parenti and Soeroto, *O. orthognathus* Kottelat, and *O. nigrimas* Kottelat, are endemic to Lake Poso (Kottelat 1990; Parenti and Soeroto 2004). The age of this lake is estimated to be 1–2 million years (Myr) (Rintelen et al. 2004; Rintelen and Glaubrecht 2006). The mtDNA phylogenies suggested that these three species are monophyletic (Fig. 4) (Mokodongan and Yamahira 2015a, b). Their complete endemism and monophyly imply that they diverged in sympatry within the lake. Because the three species could be collected at the same time from a single site on the lake (see Materials and methods, below), the first criterion of sympatric distributions (criterion i) by Coyne and Orr

(2004) is satisfied. However, the other three criteria by Coyne and Orr (2004) have not been examined rigorously. Especially, no study has yet demonstrated genetically-based reproductive isolation among the three species (criterion ii) or the absence of a historical phase of geographic isolation during their divergence (criterion iv).

In this chapter, I present evidence consistent with the hypothesis that the three *Oryzias* species in Lake Poso diverged within the lake. First, I show that these three sympatric species are valid morphological and biological species that are reproductively isolated from each other, using morphologies and population-genomic analysis of genome-wide single-nucleotide polymorphisms (SNPs). Second, I confirm that three species are monophyletic and sisters to the outgroup through phylogenetic analysis of the genome-wide SNP data. Third I demonstrate the absence of historical allopatric phase by approaches using molecular clocks for mtDNA sequences and demographic modeling of coalescence events.

2.2 MATERIALS AND METHODS

2.2.1 Field Collections

Oryzias nebulosus is sedentary species associated with shallow littoral areas with a rocky or cobbled substrate. In contrast, *O. nigrimas* and *O. orthognathus* are migratory species that are less associated with littoral areas. Consequently, specimens of *O. nebulosus* could be captured using either a beach seine during daytime or by light fishing at night, whereas daytime use of a beach seine was not efficient for collecting *O. nigrimas* and *O. orthognathus*.

I collected seven individuals of *O. nebulosus*, 20 individuals of *O. orthognathus*, and 19 Individuals of *O. nigrimas* at Saluopa, on the northwestern coast of Lake Poso (S01°47′ 08″, E120°32′12″) (Fig. 5), using a single day's catch from light fishing (see also Supplementary Methods and Results). Additionally, 20 individuals of *O. nebulosus* were collected at Dumulanga, on the southwestern coast of Lake Poso (S01°57′32″, E120°33′46″)

(Fig. 5), using a beach seine during the daytime on a different day. I also collected 20 individuals of *O. soerotoi* from Lake Tiu, using landing nets. The collected fish were preserved in 99 % ethanol after being euthanized with MS-222.

I randomly picked individuals out of the catch and later assigned each of them as one of the three species; no individual was discarded by reason of intermediate morphology. I caught only *O. nebulosus* at Dumulanga because collecting was done only during the daytime with a beach seine; however, through underwater observations I confirmed the presence of all three species at that site. Likewise, I observed the presence of all three species at Tentena, on the northeastern shore (Fig. 5).

Beach-sine nets are efficient for sampling not only lacustrine but also riverine adrianichthyids (e.g., Mandagi et al. 2018; Mokodongan et al. 2018); therefore, I employed beach seines along three rivers flowing into Lake Poso (Fig. 5), in an effort to collect as yet any undiscovered riverine adrianichthyids. However, none were found despite intensive searches. Similar field collections were also tried in the Poso River, the only drainage of Lake Poso (Fig. 5), but no adrianichtyids were found.

2.2.2 Morphological Analyses

To find possible hybrid individuals, I measured each of the 66 individuals collected from Lake Poso (19 *O. nigrimas*, 20 *O. orthognathus*, and 27 *O. nebulosus*) for standard length (SL) and body depth (BD), using a digital caliper (see also Supplementary Methods and Results). The effects of SL, species, sex and their interactions on BD were tested by fitting a linear model, using the In and anova functions in R version 3.5.1 (R Development Core Team 2014). I also counted the number of scales along the lateral midline and the number of pectoral-fin rays for each specimen under a dissecting microscope (Leica, MZ6), and counts of anal-fin rays and vertebrae were obtained from radiographs produced by soft X-ray

apparatus (Softex, E-3) (see Supplementary Methods and Results). Principal component analysis (PCA) was performed on these meristic data, and two-factor analysis of variance (ANOVA) with species, sex, and their interaction as fixed factors was performed on the PC1 and PC2 values, using the procomp and anova function in R.

2.2.3 Mitochondrial DNA Sequencing

Total DNA was later extracted from muscle samples from each of the 86 individuals (19 *O. nigrimas*, 20 *O. orthognathus*, 27 *O. nebulosus*, and 20 *O. soerotoi*) using a DNeasy Blood & Tissue Kit (Qiagen, Venlo, The Netherlands) following the manufacturer's protocol. Two mtDNA gene regions, the NADH dehydrogenase subunit 2 (ND2) and cytochrome b (cyt *b*), were amplified for each sample by Polimerase Chain Reaction (PCR) and then Sanger-sequenced, using the methods and primers described by Mokodongan and Yamahira (2015a). All sequences were aligned separately for ND2 and cyt *b*, using the Clustal W option in MEGA7 version 7.0.26 (Kumar et al.2016), and the alignment was later corrected manually. The aligned sequences of ND2 (1,053 bp) and cyt *b* (1,141 bp) were concatenated into a single sequence. Seventy-eight unique haplotypes were detected among 86 concatenated sequences, using DnaSP version 5.10.01 (Librado and Rozas 2009).

2.2.4 ddRAD Sequencing

For each of the 86 samples, genomic data were generated using double-digest restriction-site associated DNA sequencing (ddRAD-seq), with minor modifications from Peterson et al. (2012), in which *Bgl*II was used as the first restriction site adjacent to the binding site of the primer to read a single-end sequence, and *Eco*RI was used as the second restriction site adjacent to the binding site to read an index sequence (Sakaguchi et al. 2015). DNA library preparation was composed of five steps. First, restriction enzyme digestion and adapter

ligation were performed in a 10-μl reaction mixture comprising 2 μl of sample DNA (20ng/μl), 0.5 μl of *Eco*RI (10 U/μl; Takara, Osaka, Japan), 0.5 μl of *Bgl*II (10 U/μl; Takara), 1 μl of 10X NEBuffer 2 (New England Biolabs, Ipswich, MA, USA), 0.1 μl of 100X BSA (Takara), 0.4 μl of *Eco*RI adaptor (5 μl), 0.4 μl of *Bgl*II adaptor (5 μM), 0.1 μl of ATP (100 mM), 0.5 μl of T4 DNA Ligase (600 U/μl; Enzymatics, Beverly, MA, USA), and 4.5 μl of nuclease-free water. Digestion and ligation were performed at 37°C for 16 h.

The two Y-shaped adapters were prepared by annealing two partially complementary oligo-DNAs. A mixture of 100 μM adapter F and R were annealed using a thermal cycler with the following program: 95°C for 2 min, slow-cooled to 25°C (0.1°C/s), followed by 30 min at 25°C. The annealed adapter (50μM) was stored at -20°C, and then diluted to the working concentration (0.4μM) just before use. The oligo-nucleotide sequences of the Y-shaped adapters were as follows: *Bgl*II_adaptor_F: 5′-A*A*T GAT ACG GCG ACC ACC GAG ATC TAC ACT CTT TCC CTA CAC GAC GCT CTT*C*C-3′; *Bgl*II_adaptor _R: 5′-G*A*T CGG AAG AGC TGT GCA GA*C*T-3′; *Eco*RI_adaptor_F: 5′-/Phos/A*A*TTGAGATCGGAAGAGCACACGTCTGAACTCCAGTC*A*C-3′; and *Eco*RI_adaptor_R: 5’-G*T*C AAG TTT CAC AGC TCT TCC GAT C*T*C-3′, where *signifies a phosphorothioate bond and “/Phos/” signifies phosphorylation. The ligation product was purified using AMPure XP beads (Beckman Coulter, Brea, CA, USA) as follows: 10μl of AMPure XP and 10μl of ligation product were mixed after pipetting and kept at room temperature for 5 min. Purification was performed in accordance with the manufacturer’s instruction. The purified adapter-ligated DNA was subsequently amplified by PCR. Amplification was performed in 10μl reactions: 2μl of DNA, 2μl of index primer (5μM), 1μl of TruSeq_Univ_primer (10μM), 5 μl 0f 2x KAPA HiFi HotStart Ready Mix (KAPA Biosystems). The PCR was executed as follows: 94°C for 2 min and 20 cycles of 98

°C for 10 s, 65°C for 15 s, and 68°C for 15 s. the PCR product was held at 4°C. The oligo-nucleotide sequences of the primers were as follows: TruSeq_Univ_primer: 5′-AAT GAT ACG GCG ACC ACC GAG ATC TAC ACT CTT TCC CTA CAC GA-3′; and index primer: 5′-CAA GCA GAA GAC GGC ATA CGA GAT XXX XXX CTG ACT GGA GTT CAG ACG TGT-3′, where "XXXXXX" signifies and index sequence. The Index primers contained variable 6-mer index sequences that allowed multiple samples to be read in a single HiSeq lane. To distinguish the samples, different index primers were used for different samples. The PCR products of all samples were combined and concentrated using AMPure XP beads. The combined PCR product was mixed with an equal volume of AMPure XP. The mixture was kept at room temperature for 6 min, with vortexing. Then mixture was placed on a magnet, and after 5 min the supernatant was removed. The remaining beads were washed by adding 75% EtOH in excess volume to the mixture and removing the supernatant after 30 s; this was repeated twice on the magnet. After addition of 50μl of nuclease-free water, the beads were resuspended by pipetting and kept at room temperature for 1 min. the concentrated DNA was obtained by collecting the supernatant and then purified by size selection using E-Gel SizeSelect 2% agarose (Life Technologies, Carlsbad, CA, USA). Approximately 350-bp fragments were retrieved; their concentration was measured using a QuantiFluor dsDNA System (Promega, Madison, WI, USA), and the quality was measured with Bioanalyzer High Sensitivity DNA Kit (Agilent Technologies, Santa Clara, CA, USA). After preparation of the library, 50-bp sequences of either side of the DNA fragments were read using a HiSeq2500 system (Illumina, San Diego, CA, USA). The sequenced reads were demultiplexed by CASAVA 1.8.2 (Illumina).

Sequence trimming was performed using Trimmomatic version 0.32 (Bolger et al. 2014) to remove adapter regions from the illumine reads using the following settings: ILLUMICLIP:TruSeq3-SE.fa:2:30:10, LEADING:19, TRAILING:19,

SLIDINGWINDOW:30:20, and AVGQUAL:20, MINLEN:51. The remaining reads were mapped to an in-house genome assembly of an individual of *O. celebensis* (Ansai et al. 2021), using Stampy version 1.0.32 (Lunter and Goodson 2011) with the default settings. During preliminary genotyping, we found that one individual of *O. nebulosus* (*O. nebulosus* DM-17) and two individuals of *O. nigrimas* (*O. nigrimas* SL-13 and SL-17) tended to contain many missing data, probably because of the relatively small numbers of raw reads (only 0.6, 0.9, and 1.1 million reads, respectively), and that one individual of *O. nigrimas* (*O. nigrimas* SL-15) exhibited abnormally larger numbers of heterozygous sites, probably due to genomic contamination during library preparation.

After removing those four individuals, genotyping was conducted using the Stacks version 1.46 software pipeline (*pstacks, cstacks, sstacks*) (Catchen et al. 2011, 2013) with the default settings, except for the minimum of 10 reads (m=10) to create a "stack". The stacks *populations* script was used to filter the loci for those that occurred in all four species (p=4) and in all individuals of each species (r=1), where loci containing multiallelic SNPs were removed as the default setting. Genotype outputs were created in a VCF format for all SNPs per locus, and in VCF and TreeMix formats for only the first SNP per locus (write_single_SNP) with no filtering of SNP loci by allele frequency. Exact test of Hardy-Weinberg equilibrium (HWE) (Wigginton et al.2005) was performed separately for each species, using VCFtools version 0.1.13 (Denecek et al. 2011), and the loci deviating from HWE (1% significance level) in one or more species were excluded from the dataset. Finally, 3,188 RAD-loci, including 2.718 SNP loci, were obtained for all 82 individuals, with no missing data. In addition, a PHYLIP file of concatenated sequences was created for loci that occurred in all 82 individuals, using the *populations* script (p=82, r=1, and phylip_var_all). Exclusion of the above loci deviating from HWE resulted in 3,079 loci, with a total length of 157,029 bp, including both variant and invariant sites.

2.2.5 Phylogenetic Analysis

Phylogenies were constructed separately for the concatenated mitochondrial genes and the concatenated RAD sequences, using maximum likelihood (ML) methods. For mtDNA data set, a phylogeny among the 78 unique mitochondrial haplotypes was estimated using raxmlGUI version 1.31 (Silvestro and Michalak 2012), where the codon-specific GTRGAMMA model was used. Sequences of *O. soerotoi* were treated as outgroups, and bootstrap replicates. For the 157,029-bp concatenated RAD-sequences, a Neighbor-Joining (NJ) tree was reconstructed, using p-distances. Analysis was performed with MEGA7, where a bootstrap analysis of 1,000 bootstrap replicates was conducted.

For the RAD-seq 2,718 SNP dataset, also built individual-based phylogenetic networks using SplitsTree version 4.14.6, build 26 (Huson and Bryant 2006). The networks were built using the Neighbor-Net method based on Nei's standard genetic distances between individuals (Nei 1972), which were calculated from the individual genotype calls, using the R package StAMPP version 1.5.1 (Pembleton et al. 2013).

A species tree was also built for the RAD-seq SNP dataset, using Bayesian estimation implemented with SNAPP version 1.4.1 (Bryant et al. 2012), an add-on package of BEAST version 2.5.0 (Bouckaert et al 2014). The VCF file was reduced into five randomly selected individuals per species, using VCFtools. Backward (U) and forward (V) mutation rates were estimated from the stationary allele frequencies in the data (U=14.0344, V= 0.5185). Analysis was run using default priors with chainLength = 1000000 and storeEvery = 1000. Markov-chain Monte Carlo (MCMC) convergence to the stationary distribution and a large effective sample size (ESS >200) were confirmed for all parameters, using Tracer version 1.6.0 (Rambaut et al. 2014). We discarded the first 25% of the trees as burn-in and visualized the posterior distribution of the remaining 750 trees as consensus trees using DensiTree

version 2.2.6 (Bouckaert 2010).

2.2.6 Population-Structure Analysis

To examine population structure, principal component analyses (PCA) were conducted based on the RAD-seq 2,718 SNP dataset, using R package SNPrelate version 1.10.2 (Zheng et al. 2012). Admixture analysis was conducted using ADMIXTURE version 1.3.0 (Alexander et al. 2009), based on a PED file converted from the VCF file, using PLINK version 1.90b4.6 (Purcell et al. 2007). ADMIXTURE was run for 1-5 clusters. Statistical support for the different number of clusters was evaluated based on five-fold cross-validation implemented in ADMIXTURE.

2.2.7 Divergence-Time Estimation

Lognormal relaxed clock analyses were performed in BEAST version 2.5.0 (Bouckaert et al.2014) on the mtDNA sequence dataset. Analysis was run by partitioning the codon positions for both ND2 and cyt *b*. Appropriate substitution models for each codon were determined (Table 1) using jModel Test version 2.1.7 (Darriba et al. 2012). Regarding the molecular clocks of Adrianichthydae, Stelbrink et al. (2012) estimated the time to the most recent common ancestor (TMRCA) of the Sulawesi adrianichthyds using substitution of 2.5%-3.1% per Myr for ND2, which had been estimated for a pupfish (Echelle et al. 2005). Alternatively, Takehana et al. (2003) estimated the divergence times of major lineages of Japanese *Oryzias* using substitution rates of 2.5%-2.8% per Myr for cyt *b*, which had been previously estimated for sticklebacks (Orti et al. 1994) and a goby (Harada et al. 2001). In this study, I used a substitution rate of 2.80% (the median of 2.5%-3.1%) per Myr for ND2, and 2.65% (the median of 2.5%-2.8%) per Myr for cyt b. The other settings were as follows: Yule Model, chainLength = 800000000 and logEvery = 1000. Convergence of the MCMC to

the stationary distribution and a large ESS (>200) were confirmed for all parameters using the Tracer program, after discarding the first 20% generations as burn-in.

2.3 RESULTS

2.3.1 Morphology

For all species, each individual exhibited typical secondary sexual characteristics in fin shape and body coloration, and could be sexed, indicating that they had matured. After correcting for SL, the *O. nebulosus* individuals were found to be deeper-bodied than the *O. nigrimas* and *O. orthognathus* individuals (Fig. 6A). the ANOVA revealed that the effect of species on body depth (BD) and the interaction between SL and species were significant (Table 2). Sexual difference in BD was non-significant (Table 2), though males tended to be deeper-bodied than females in *O. nebulosus*. The interaction term between SL and sex was also significant, indicating a sexual difference in the allometry of BD.

All four meristic characters very more or less among the three species (Table 3). Especially, the number of scales along the lateral midline greatly differed among the three species: *O. orthogntahus* had 52-54 scales (mean 53.5), whereas *O. nebulosus* had 33-35 (mean 34.4) and *O. nigrimas* had 36 or 37 (mean 36.3) (Table 3). The principal component (PC) analyses revealed that 56.4% and 27.8% of the variance in these meristic characters were explained by PC1 and PC2, respectively. A scatter plot of the PC1 and PC2 scores showed distinct clusters for the three species (Fig 6B), where PC1 separated all three species from each other, while PC2 separated *O. nigrimas* from the other two species. ANOVA revealed that the effect of species was significant both in PC1 and PC2, but that the effect of sex and the interaction between species and sex were non-significant in both (Table 4).

2.3.2 Phylogeny

The ML phylogeny based on the 78 unique mitochondrial haplotypes detected from among the 86 individuals supported the monophyly of the Poso species complex with ML bootstrap (MLB) = 100% (Fig. 7A). Two major clades were evident within the Poso clade, one of which comprised *O. nigrimas* (MLB = 99%), and the other was a mixture of *O. nebulosus* and *O. orthonathus* (MLB = 100%).

The NJ nuclear phylogeny based on the 157,029-bp concatenated RAD sequences for the 82 individuals also revealed the monophyly of the Poso species complex (Fig. 7B). However, unlike in the mtDNA phylogeny, the three species tended to be clearly separated from each other. Especially, *O. nebulosus* and *O. orthognathus* formed a clade.

Neighbor-Net phylogenetic network based on the 2,718 SNPs also supported the monophyly of the three species (Fig. 8). As in the ML nuclear phylogeny, the three species were clearly separated from each other. Within the Poso clade, *O.nigrimas* was split at first, followed by the split between *O. nebulosus* and *O.orthognathus*.

The species tree estimated by SNAPP also yielded the same topology (Fig. 9). In the posterior distribution of the three species trees, all of the trees supported a topology consistent with the NJ tree and the above phylogenetic network.

2.3.3 Population Structure

The ADMIXTURE analysis revealed that the occurrence of three clusters (K = 3) had the highest support (Fig. 10). In the case of K = 4, the three species in Lake Poso (i.e., *O. nebulosus*, *O. orthognathus*, and *O. nigrimas*) and *O. soerotoi* in Lake Tiu were clearly separated from each other (Fig. 11). One individual of *O. nebulosus* exhibited a small sign of admixed ancestry with *O. orthognathus*. In the case of K = 3, *O. nebulosus* and *O. orthognathus* became one single population (Fig. 11). Two *O. nebulosus* populations (Saluopa and Dumulanga) were not distinguishable even when K = 5.

Four distinct clusters were also apparent in the PCA (Fig. 12). The first principal component (PC1) clearly differentiated the Poso species from *O. soerotoi*, whereas the three Poso species were differentiated from each other by the second and third principal components (PC2 and PC3).

2.3.4 Divergence Time

Using the molecular clocks for ND2 and cyt *b*, the TMRCA of the Poso species complex and *O. soerotoi* in Lake Tiu was estimated to be 1.38–2.91 Mya (mean=2.11 Mya), which was in the early-mid Pleistocene (Fig. 13, node 1). Within the Poso clade, *O. nigrimas* was estimated to have diverged at 0.96–1.98 Mya (mean=1.45 Mya) (Fig. 13, node 2). The other two Poso species, *O. nebulosus* and *O. orthognathus*, were not separated in the Bayesian-inferred phylogeny as well. The first diversification of *O. nebulosus*-*O.orthognathus* haplotypes occurred at about 0.49-1.05 Mya (mean=0.75 Mya) (Fig. 13, node 3).

2.4 DISCUSSION

Theories predict that sympatric speciation is possible under certain conditions (e.g., Dieckmann and Doebeli 1999; Higashi et al. 1999; Kondrashov and Kondrashov 1999; Bolnick and Fitzpatrick 2007). However, only a few empirical case studies demonstrating this mode of speciation are available (Coyne and Orr 2004; Bolnick Fitzpatrick 2007). Our results suggest that three sympatric species of *Oryzias* in Lake Poso, *O. nigrimas*, *O. nebulosus*, and *O. orthognathus*, have diverged within the lake in sympatry.

2.4.1 Monophyly and Reproductive Isolation of Sympatric Species

The phylogenetic sister relationship among the three Poso species, which is one of the criteria given by Coyne and Orr (2004) for sympatric speciation, was clearly re-demonstrated in this

study. Their monophyly was supported by mtDNA phylogenies as well as by genome-wide SNP-based phylogenies.

We also present evidence for reproductive isolation among the species, which is another criterion for sympatric speciation (Coyne and Orr 2004). The three species are clearly distinguishable from each other by a combination of only a few morphological characters (i.e., body depth and several meristic characters), suggesting no ongoing hybridization. The ADMIXTURE analysis, PCA, and the phylogenetic analyses based on the SNPs also support the hypothesis that they are reproductively isolated from each other. Although mtDNA phylogenies failed to separate *O. nebulosus* and *O. orthognathus*, this may reflect incomplete lineage-sorting. Indeed, our ADMIXTURE analysis revealed that these two species were clustered as a single population in the case of K= 3, indicating that they are genetically very close to each other. However, they were clearly separated when K = 4. We conclude that *O. nebulosus* and *O. orthognathus* are reproductively isolated biological species, but that they are still young species that have diverged recently (see below for a discussion on their divergence time).

It is unclear, however, how the tree species are reproductively isolated from each other in the wild. I observed underwater that there might be a partial difference in mating habitats; during the course of field collections, I discovered a mating habitat, a shallow (<1 m) littoral area in Dumulanga composed of cobbles, which was shared by *O. nebulosus* and *O. orthognathus* but never by *O. nigrimas*. Then again, I do not know where *O. nigrimas* and the other two species might reflect the difference in mating habitats, which is the case in several species of Cameroon crater lake cichlids (Martin 2012), though *O. nebulosus* and *O. orthognathus* have apparently evolved reproductive isolation despite sharing mating habitats. Further, investigations on prezygotic and postzygotic isolations are necessary to clarify the mechanisms of reproductive isolation among the three sympatric species.

2.4.2 No Historical Phase of Geographic Isolation During Speciation

Our mtDNA chronogram revealed that the TMRCA of the Poso *Oryzias* and *O. soerotoi* in Lake Tiu (1.38–2.91 Mya) largely overlaps with the age of Lake Poso (1–2 Mya) (Rintelen et al. 2004; Rintelen and Glaubrecht 2006). This does not contradict the scenario that the divergence between the Poso *Oryzias* and *O. soerotoi* occurred in allopatry. Lake Poso is a cone-shaped tectonic lake (Surface area: 323 km^2) where the center of the lake is the deepest (maximum 450 m) (Abendanon 1915; see also Rintelen et al. 2012 and Fig. 2 for a bathymetry map), suggesting no historic phase during which the lake was separated into two or more parts by water-level changes. Therefore, it is reasonable to consider that endemic species there have diverged within the lake, when their divergence time was estimated to be younger than the age of the lake. Although cautions are needed because the age estimate for this lake is relatively preliminary (Rintelen et al. 2004), it appears that *O. nebulosus* and *O. orthognathus* diverged after the formation of Lake Poso, because the coalescent time of mitochondrial haplotypes of these two species was estimated to be about 0.75 Mya (0.49–1.05 Mya), and their population divergence probably postdated this. Overall, all of these estimates support that there was no allopatric phase during their divergences.

2.4.3. A new case example of sympatric speciation

Theories predict that sympatric speciation is possible under certain conditions (e.g., Dieckmann and Doebeli 1999; Higashi et al. 1999; Kondrashov and Kondrashov 1999; Bolnick and Fitzpatrick 2007). However, only a few empirical case studies demonstrating this mode of speciation are available (Coyne and Orr 2004; Bolnick and Fitzpatrick 2007). The results obtained in this study were all concordant with the four criteria for sympatric

speciation suggested by Coyne and Orr (2004). Thus, I conclude that the three Poso *Oryzias* species are a new clear addition to empirical examples of sympatric speciation in the wild.

CHAPTER 3

RESOURCE PARTITIONING AND ASSORTATIVE MATING

3.1 INTRODUCTION

Sympatric speciation is considered to be possible under limited conditions (e.g., Higashi, Takimoto, and Yamamura, 1999; Kondrashov and Kondrashov, 1999; Dieckmann and Doebeli, 1999; Bolnick and Fitzpatrick, 2007). However, empirical studies have demonstrated that sympatric speciation does occur in the wild (e.g., Schliewen, Tautz, and Paabo, 1994; Sorenson, Sefc and Payne, 2003; Herder et al. 2006; Savolainen et al. 2006; Sutra et al. 2019; see Bolnick and Fitzpatrick 2007, for review). Therefore, the conditions required for sympatric speciation have long intrigued many evolutionary biologists (e.g., Mayr, 1963; Futuyma and Mayr, 1980; Berlocher and Feder, 2002; Coyne and Orr, 2004; Foote, 2018; Richards, Servedio and Martin, 2019).

Theories predict that sympatric speciation generally requires both resource partitioning by disruptive selection and assortative mating by mate preference and/or spatial or temporal reproductive isolation (Felsentein, 1981; Dieckmann and Doebeli, 1999; Kondrashov, 1999; Doebeli et al., 2005). The major obstacle to sympatric speciation is that the recombination would erode the coupling between the ecological traits that allow resource partitioning and the reproductive traits that allow assortative mating (Dieckmann and Doebeli et al., 2005; Kopp et al., 2018). Therefore, it is predicted that ecological traits and reproductive traits should be coupled with each other in some way (Dieckmann and Doebeli et al., 2005; Kopp et al., 2018). The most intelligible case is that utilization of different resources automatically leads to assortative mating as a byproduct (Servedio et al., 2011). It is proposed that such an “automatic magic trait” is a requirement for the completion of sympatric speciation (Martin, 2013; Martin et al., 2015).

Population genomic analyses of genome-wide single-nucleotide polymorphisms (SNPs) showed that these three *Oryzias* species diverged in sympatry within the lake (Fig. 11; Sutra et al. 2019). The three species are reproductively quite isolated from another, indicating that sympatric speciation has been completed. Sutra et al (2019) reported that spatial isolation partly contributed to their assortative mating: *O. nigrimas* never shares a breeding site with *O. nebulosus* and *O. orthognathus*. However, details of the assortative mating of these three species are yet to be investigated. How these three species use different resources in the lake is also unknown.

In this chapter, I first investigated the lake-wide population structures of the three species of *Oryzias* in Lake Poso using genome-wide SNPs, and demonstrate that they are reproductively isolated throughout the lake. Second, to clarify the manner of resource partitioning among the three species, I compared their feeding morphologies and trophic niches based on carbon and nitrogen stable isotope analyses. Third, to see how assortative mating is achieved, I examined several reproductive traits, including egg characteristics and mating behaviors. On the basis of these results, I tested whether both resource partitioning and assortative mating have evolved among these species, as predicted by theories of sympatric speciation, and assess the contribution of magic traits to their sympatric divergence within this ancient lake.

3.2 MATERIAL AND METHODS

3.2.1 Field Collections and Underwater Observations

I collected *Oryzias* species from Lake Poso at Tentena, Taipa, Pendolo, Tolambo, and Peura (Fig. 14), using night time light fishing and/or a beach seine net during the day time (Table 5). In total, 31, 39, and 33 individuals of *O. nigrimas*, *O. orthognathus*, and *O. nebulosus* were collected, respectivel, and preserved in 99% ethanol (Table 5). I also collected 10 males and

10 females each of *O. nigrimas* and *O. orthognathus* at Tentena and 10 males and 10 females of *O. nebulosus* at Dumulanga and preserved them in 5% formalin (Table 5).

I made underwater observation by snorkeling during the daytime at Tentena and Dumulanga. I observed all three species at Tentena, whereas only *O. nebulosus* and *O. orthognathus* were found at Dumulanga.

3.2.2 Population structural analyses

Among the individuals preserved in ethanol, 11 *O. nigrimas*, 19 *O. orthognathus*, and 13 *O. nebulosus* individuals (Table 5) were processed for double-digest restriction-site-associated DNA (RAD) sequencing (ddRAD-seq) (Peterson et al. 2012; see Sutra et al (2019) for details of library preparation). The library was sequenced with 150-bp paired-end reads on an Illumina HiSeqX system (Illumina, San Diego, CA, USA) by Macrogen Japan Corporation (Kyoto, Japan). Raw ddRAD-seq (50-bp single-end) reads for each of the 16 *O. nigrimas*, 20 *O. orthognathus*, and 26 *O. nebulosus* individuals (Table 5) were also obtained from DDBJ Sequence Read Archive (DRA007977).

The ddRAD-seq reads were trimmed to remove adapter sequences and failed reads using Trimmommatic version 0.39 (Bolger et al. 2014), with the following parameters: TruSeq3-PE-2.fa:2:30:10:2 LEADING:3 TRAILING:3 SLIDINGWINDOW:4.20 MINLEN:51. The trimmed forward reads were mapped to the genome assembly of an *O. celebensis* individual (OryCel_1.0) (Ansai et al. 2021) using Stampy version 1.0.32 (Lunter and Goodson, 2011). Genotyping was conducted with the *ref_map.pl* pipeline of Stacks version 2.54 (Rochette, Rivera-Colon, and Catchen, 2019), with the default settings. The *population* program of Stacks was used to export a VCF file. I removed the genotypes with read depths of < 10 using BCFtools version 1.9 (Li, 2011). Loci that deviated from Hardy-Weinberg equilibrium ($P < 0.01$) or were missing in more than 10% of the individuals in any

species were excluded from the dataset using VCFtools version 0.1.17 (Danecek et al. 2012). If an allele at a SNP site was found in only one individual, identified as a “singleton” or “doubleton” by the *singleton* function of VCFtools, the SNP site was removed. The SNPs were subsampled with VCFtools to maintain a minimum distance of 1 kb in order to reduce the effect of linkage between SNPs. This resulted in 1,879 biallelic SNPs.

I examined the population structures within and among the three species with ADMIXTURE version 1.3.0 (Alexander, Novembre, and Lange, 2009). ADMIXTURE was run for 1–4 clusters (i.e., $1 \leq K \leq 4$). Statistical support for the different numbers of clusters was evaluated with the cross-validation technique implemented in ADMIXTURE. The results were summarized and visualized with CLUMPAK web pipeline (Kopelman et al. 2015; http://clumpak.tau.ac.il/index.html). I also conducted a principal components analysis (PCA) using the adegenet version 2.1.1 package (Jombart, 2008; Jombart and Ahmed, 2011) of *R* (R Core Team, 2020)

3.2.3 Morphological analyses

The individuals preserved in formalin were photographed separately from the right side with a ruler, using a digital camera (EOS 60D, Canon, Tokyo, Japan), for geometric morphometric shape analysis. The digital pictures were later transferred to a personal computer, and 15 landmarks were placed, according to Mokodongan et al. (2018), on the images using the image analysis software Inkscape version 0.92 (https://inkscape.org). A generalized Procrutes analysis was conducted on landmark coordinates to adjust the scale and placement of objects, and PCA was performed on the Procrustes superimposed coordinates, using MorphoJ version 1.06d (Klingenberg, 2011).

After each individual was photographed, it was dissected and the digestive tract and gills were removed. The digestive tract was stretched under a dissecting microscope (Leica,

MZ6) and photographed with a digital camera. The length of each digestive with Inkscape. The first left gill arch was removed and photographed with a dissecting microscope camera system equipped with an objective micrometer (Leica, MZ6 with iPhone 8). The length of each gill raker and the interval between adjacent gill rakers were then measured with Inkscape (Fig. 15).

3.2.4 Stable isotope analyses

Among the individuals preserved in ethanol, 10 males and 10 females of both *O. nigrimas* and *O. orthognathus* collected from Taipa and 10 males and 10 females of *O. nebulosus* collected from Dumulanga were processed for stable isotope analyses. The caudal muscle was dissected from each fish, dried for 48 h at 60 ºC, and ground. The ground samples were placed in chloroform-methanol (2:1) solution to remove the lipids and redried. The stable isotope rations for carbon and nitrogen were measured with a continuous-flow isotope ratio mass spectrometer (CF/IRMS; DELTA V advantage, Thermo Fisher, Germany). The isotope ratios were expressed as the per mil deviation from the standard, as follows:

$\delta^{13}C$ or $\delta^{15}N = (R\text{sample}/R\text{standard} - 1) \times 1000$ (‰)

where $R = {}^{13}C/{}^{12}C$ or ${}^{15}N/{}^{14}N$. Vienna Pee Dee belemnite and atmospheric nitrogen were used as the standards for carbon and nitrogen, respectively. The analytical precisions based on the working standards (Tayasu et al. 2011) were ±0.10‰ and ±0.14‰ for $\delta^{13}C$ and $\delta^{15}N$, respectively.

3.2.5 Measurement of egg characteristics

Several live individuals of the three Poso *Oryzias* species were transported to our laboratory (World Medaka Aquarium, Nagoya Higashiyama Zoo and Botanical Gardens, Nagoya, Japan) and bred in aquaria (water temperature 26º C; 13 h light: 11 h dark cycle). I tested

whether the females of the three species attached fertilized eggs to submerged materials or scattered them around the bottom in the following aquarium experiments. First, one female and one male of each species were transferred to one of three acrylic tanks. Each tank had a bunch of yarn suspended and a raised bottom with a mesh screen (30 × 25 × 20 cm water depth about 20 cm). The presence or absence of fertilized eggs on the yarn and below the raised bottom was checked in the afternoon everyday this observation was repeated until eggs were found three times (i.e., on the three days) for each species.

I also collected fertilized eggs *O. nigrimas* from the yarn and preserved them in 5% formalin. The eggs of *O. orthognathus* and *O. nebulosus* were collected directly from females carrying fertilized eggs. Digital pictures of the eggs were taken with a dissecting microscope camera system equipped with an objective micrometer (Leica, MZ6 with DFC320, and the diameter of each egg was measured with Illustrator CS6 version 16.0.4 (Adobe, San Jose, CA, USA) with BPT-Pro2 (Baby, Universe, Fujisawa, Japan).

3.2.6 Mating experiments

The following mating experiment were conducted with *O. orthognathus* and *O. nebulosus*, which share a breeding site in the wild (see Results). I randomly chose three adult males and three adult females from each of the aquaria containing the *O. orthognathus* and *O. nebulosus* populations. On the evening before each mating trial, one male and one female were transferred to a temperature and photoperiod-controlled tank (30 × 25 × 20 cm, water depth about 20 cm) and separated into the right and left of the tank by an opaque acrylic wall. On the next morning (at approximately 09:30), the day's session of mating experiments was initiated by opening the wall. The male and female were allowed to mate freely. I recorded their behavior until around 14:00 using digital video cameras (FDR-AX45, Sony, Tokyo, Japan). The males and females were left free and fed brine shrimp nauplii and dry feed until

the evening, when the males and females were separated again by the acrylic wall for the next day's session. This trial was repeated three times for each of all combinations of males and females, using three males and three females of the same species (*O. orthognathus* males × *O. orthognathus* females and *O. nebulosus* males × *O. nebulosus* females) or from different species (*O. orthognathus* males × *O. nebulosus* females and *O. nebulosus* males × *O. orthognathus* females).

Both the males and females of *O. nebulosus* and *O. orthognathus* become black in breeding mood (see Results). I tracked the body color changes in the males and females until spawning or until the end of the Day's session. When spawning occurred, I also recorded the time until spawning.

3.2.7 Statistical analyses

Interspecific differences in the first and second principal components (PC1 and PC2, respectively) of the geometric morphometric shape analysis, the number of gill rakers, the $\delta^{13}C$ and $\delta^{15}N$ values in the stable isotope analyses, and the egg diameters were tested with analysis of variance (ANOVAs), with species as the fixed factor, followed by pairwise comparisons with Tukey's HSD test. Interspecific differences in the elevations (intercepts) of the regression lines of digestive tract length (log-transformed) against standard length (SL; log-tranformed) were tested with analysis of covariance (ANCOVA), with species as the fixed factor and standard length as a covariate, followed by pairwise comparisons with Tukey's HSD test. Interspecific differences in gill raker lengths and gill raker intervals were tested with three-way ANOVA using the first to 14th gill rakers of the three largest individuals, with the species and the gill raker lengths and intervals as the fixed factors and the individual as the random factor. The differences in the time until spawning after mating with a conspecific male versus after mating with a male of a different species were tested

separately for *O. nebulosus* females and *O. orthognathus* females with two-way ANOVA, with male species as the fixed factor and the individual female as the random factor. These tests were performed with JMP version 13.2.0 (SAS Institute, Cary, USA). The frequencies obtained in the mating experiments were tested with a χ^2 test.

3.3 RESULTS

3.3.1 Intra-lake population structure

The ADMIXTURE analysis of the three *Oryzias* species, *O. nebulosus*, *O. orthognathus*, and *O. nigrimas*, collected throughout the lake revealed that the occurrence of three clusters (K = 3) had the highest support (Fig. 17). The three species were clearly separated from each other, irrespective of the collection site (Fig. 14). The three species were also separated from each other by PC1 and PC2 of the PCA (Fig. 18).

3.3.2 Morphologies

A scatterplot of the PC1 and PC2 scores in the geometric morphometric shape analysis revealed that the three species were separated from each other (Fig. 19). The interspecific difference was significant in both PC1 and PC2 (Table 6). PC1 reflected the overall abdominal length (especially in landmarks 4, 5, 12, and 13) and head length (landmarks 3 and 14), indicating that *O. nebulosus* had a shorter abdomen and a longer head than *O. orthognathus* (Tukey's HSD test, $P < 0.001$) or *O. nigrimas* ($P < 0.001$). PC2 reflected the overall body depth (especially in landmarks 4, 5, 12, and 13), indicating that *O. orthognathus* was more slender than *O. nebulosus* (Tukey's HSD test, $P < 0.001$) and *O. nigrimas* ($P < 0.001$). The species × sex interaction was highly significant in PC2 (Table 6B), because males are deeper bodied than females in *O. nebulosus* (Tukey's HSD test, $P = 0.015$).

Individuals of *O. nebulosus* (24.8–37.8 mm SL) were generally smaller than those of *O. orthognathus* (43.8–51.4 mm SL) and *O. nigrimas* (38.0–51.1 mm SL). *Oryzias orthognathus* had a shorter digestive tract for its body size than *O. nebulosus* or *O. nigrimas* (Fig. 19). The interspecific difference in digestive tract length was significant after correction for body size (Table 7). *Oryzias orthognathus* had a significantly shorter digestive tract than *O. nebulosus* (Tukey's HSD test, $P < 0.001$) or *O. nigrimas* ($P < 0.001$), but the latter two species did not differ significantly ($P = 0.875$).

Oryzias nigrimas had a smaller gill arch for its body size than *O. nebulosus* or *O. orthognathus*; the difference in gill arch length was significant after correction for body size (Fig. 21, Table 8). *Oryzias orthognathus* had significantly more gill rakers (Table 9) than *O. nebulosus* (Tukey's HSD test, $P < 0.001$) or *O. nigrimas* ($P < 0.001$) (Fig. 19). When the three largest individuals were compared, each gill raker of *O. orthognathus* was significantly longer (Table 10A) than the corresponding gill rakers of *O. nebulosus* (Tukey's HSD test, $P < 0.001$) or *O. nigrimas* ($P < 0.001$). *Oryzias orthognathus* also had larger gill raker intervals (Table 10B) than the other two species (Tukey's HSD tests, $P < 0.001$).

3.3.3 Feeding behaviors and stable isotope analyses

I observed that under water, all three *Oryzias* species pecked in the water column of the lake. *Oryzias nebulosus* is a sedentary species associated with shallow littoral areas with rocky or cobbled substrates. It pecked in the water column at a depth of ca. 1 m at Dumulanga, a breeding site of this species (see below). In contrast, *O. orthognathus* and *O. nigrimas* are mobile species, less associated with littoral areas; they move around in the lake. We found that *O. orthognathus* and *O. nigrimas* swam in large schools and pecked in the water column at a depth of ca. 1–4 m at Tentena. None of the *Oryzias* species pecked on the bottom. The

gastric contents were greenish in *O. nebulosus* and *O. nigrimas*, but yellowish in *O. orthognathus* (Fig. 23).

Stable isotope analyses revealed that the three *Oryzias* species differed from one another in both their $\delta^{13}C$ and $\delta^{15}N$ values (Fig. 24). The interspecific differences were significant for both $\delta^{13}C$ and $\delta^{15}N$ (Table 11). *Oryzias nigrimas* showed significantly higher $\delta^{13}C$ values than *O. nebulosus* (Tukey's HSD test, $P < 0.001$) and *O. orthognathus* ($P < 0.001$). *Oryzias nebulosus* showed significantly higher $\delta^{15}N$ values than *O. orthognathus* (Tukey's HSD test, $P < 0.001$) and *O. nigrimas* ($P < 0.001$).

3.3.4 Spawning sites and egg characteristics

I identified a breeding site, a shallow (< 1 m) littoral area in Dumulanga composed of unvegetated cobbles, that was shared by *O. nebulosus* and *O. orthognathus* (Fig. 25), but never by *O. nigrimas*. The spawning of these two species was observed in the morning. *Oryzias nebulosus* also stayed at the cobble beach in the afternoon, whereas *O. orthognathus* left the beach in the afternoon. We identified no breeding site for *O. nigrimas*, despite intensive field surveys.

In the aquaria, the *O. orthognathus* and *O. nebulosus* females produced smaller eggs than the *O. nigrimas* females (Fig. 26) and the difference in egg size was significant (ANOVA, $F_{2,99} = 2109.6$, $P < 0.001$; Tukey's HSD tests, $P < 0.001$ for all species pairs). The *O. orthognathus* and *O. nebulosus* females scattered their fertilized eggs around the bottoms of the aquaria every day, whereas the *O. nigrimas* females attached their fertilized eggs to the submerged yarn. Eggs of *O. orthognathus* and *O. nebulosus* lacked adhesiveness; they never adhered fingers or tweezers when being collected unlike those of *O. nigrimas.*

3.3.5 Mating behaviors of *O. nebulosus* and *O. orthognathus*

Laboratory mating experiments revealed that the *O. nebulosus* females took longer to spawn when they mated with an *O. orthognathus* male than when they mated with a conspecific male (Fig. 27). The effect of the male species (conspecific versus heterospecific) on the spawning time was significant (Table 12). The total number of days on which the *O. nebulosus* females spawned decreased when they mated with an *O. orthognathus* male compared with when they mated with a conspecific male (9/27 versus 17/27), although the reduction was not significant ($\chi^2 = 1.678$, $P = 0.195$). Similarly, *O. orthognathus* females also tended to take longer to spawn when they mated with a male of a different species, i.e., *O. nebulosus* (Fig. 27), although the female response was not as great as that of *O. nebulosus*, as shown by the significant male species × female species interaction (Table 12). The total number of days on which *O. orthognathus* females spawned also did not decrease as much as in *O. nebulosus* when they mated with a male of a different species (9/27 versus 10/27; $\chi^2 = 0.039$, $P = 0.844$). However, in both *O. nebulosus* and *O. orthognathus*, the females never spawned on the day of the first contact when mated with a male of a different species (Table 13); this reduction in spawning occasions on the first day was significant for both *O. nebulosus* females ($\chi^2 = 6.118$, $P = 0.013$) and *O. orthognathus* females ($\chi^2 = 4.800$, $P = 0.029$).

The males of both *O. nebulosus* and *O. orthognathus* turned black when they were in breeding mood. Each day's mating session started with the male's becoming black (Table 14). The mating dance of the *O. nebulosus* males involved small movements with the head downward in front of the female, whereas the males of *O. orthognathus* swam parallel to a female, zigzagging in a vertical direction. When the females accepted the males, the females of both species also turned black, although the degree of blackness was much greater in the *O. nebulosus* females than in the *O. orthognathus* females. The males of both species sometimes became pale, losing the breeding motivation. In particular, the *O. nebulosus* males lost

breeding motivation more frequently when mated with an *O. orthognathus* female than when mated with a conspecific female (Table 14) (12/27 versus 2/27; $\chi^2 = 5.798$, $P = 0.016$). However, in most cases (9/12), the males of *O. nebulosus* recovered their breeding motivation (turned black) and completed spawning. Some *O. orthognathus* males also lost breeding motivation when mated with an *O. nebulosus* female (Table 14), but the response was not significant (0/11 versus 2/11; $\chi^2 = 1.846$, $P = 0.174$).

3.4 DISCUSSION

3.4.1 Resource partitioning among *Oryzias* in Lake Poso

Stable isotope analyses revealed that the three *Oryzias* speies occupied different trophic niches on the $\delta^{13}C$–$\delta^{15}N$ plot. Although their food resources could not be identified, based on behavioral observation, it is probable that they feed on plankton in the water column. This niche segregation probably reflects the differences in the morphologies of their gill rakers and digestive tracts and in their feeding sites. *O. orthognathus* has larger gill raker intervals and a shorter digestive tract than *O. nigrimas* and *O. nebulosus*, and the latter two differ in their feeding sites, i.e., pelagic and littoral, respectively. The laterally compressed deeper body of *O. nebulosus*, which is considered to confer greater maneuverability (Blake, 1983; Webb, 1984; Wootton, 1998; Langerhans and Reznick, 2010), may be an advantage in feeding in shallow littoral areas, which are spatially more complex than pelagic areas.

The longer digestive tracts of *O. nigrimas* and *O. nebulosus* are probably an adaptation to feeding on phytoplankton (German, 2011). The digestive tracts of these two species were filled with granular green alga (although the species were not identified). In contrast, the gut contents of *O. orthognathus* were gelatinous yellowish matter, suggesting carnivory. Because *O. orthognathus* pecked in the water column and had larger gill raker intervals, I infer that its gut contents were zooplankton. If so, the lower $\delta^{15}N$ values of

O.orthognathus compared with those of *O. nigrimas* and *O. nebulosus* contradict the general rule in aquatic food webs that $\delta^{15}N$ usually increases as the trophic level increase (McCann, Rasmussen, and Umbanhowar, 2005). A possible explanation of this phenomenon is that food resources of *O. orthognathus* derive from a different trophic pathway, in which the baseline $\delta^{15}N$ value differs from that in the trophic pathway used by *O. nigrimas* and *O. nebulosus*. Further analyses, including those of potential food items, are required to identify the food resources of the species.

3.4.2 Assortative mating *Oryzias* in Lake Poso

I found that *O. orthognathus* and *O. nebulosus* share a littoral spawning site covered with cobbles, which is never used by *O. nigrimas*. It is likely that the smaller and less adhesive eggs produced by *O. nebulosus* and *O. orthognathus* reflect an adaptation to cobbled beaches, female *O. orthognathus* and *O. nebulosus* scattered their eggs around the bottom of the aquaria, whereas *O. nigrimas* deposits its eggs on submerged material, probably aquatic plants, as in many other species of *Oryzias* (Iwamatsu, 2006). Although I did not identify the spawning site of *O. nigrimas* in the wild, it is highly probable that the breeding of *O. nigrimas* and the other two species is spatially isolated.

However, I demonstrated that strong prezygotic isolation by mate preference has evolved between *O. orthognathus* and *O. nebulosus*. In the laboratory, the females of both species tended to take longer to spawn when mated with males of the other species. Moreover, the females never spawned on the day of the first contact when mated with males of the other species. The females started to accept males of different species from the second day, when they encountered no conspecific males, but such a situation is improbable in the wild, at least at the spawning site at Dumulanga. Females probably recognize conspecific males by breeding coloration; both *O. nebulosus* and *O. orthognathus* males become blackish,

although the former is much darker. Furthermore, the lower margin of the caudal fin of the *O. orthognathus* male is orange, whereas no such caudal coloration is detectable in *O. nebulosus* males. It is also probable that the species-specific mating dance functions as another mating signal to conspecific females.

Interestingly, the males of both species also seem to show a preference for conspecific females. The males frequently lost their breeding coloration when mated with females of a different species. I consider that the body coloration of the females also functions as a mating signal to the males. The females of *O. nebulosus* become black when they accept a male, and the females of *O. orthognathus* also turn darker, but to a lesser degree. These data indicate that strong prezygotic isolation between *O. orthognathus* and *O. nebulosus* is achieved by the robust discrimination against a mate of the order species by both sexes, rather than by female mate preference alone.

3.4.3 Sympatric speciation without magic?

Sympatric speciation is considered to be difficult without the coupling between ecological traits that allow resource partitioning and reproductive traits that allow assortative mating. Such “magic traits” are known to be involved in most of the compelling examples of sympatric speciation. Therefore, I report a possible case of sympatric speciation without magic traits. Three species of ricefish (genus *Oryzias*) are known to have diverged sympatrically within Lake Poso, an ancient lake in Sulawesi. I demonstrated above that both resource partitioning and assortative mating have evolved among the three Poso *Oryzias* species, which is consistent with theories of sympatric speciation (Felsenstein, 1981; Dieckmann and Doebeli, 1999; Kondrashov and Kondrashov, 1999; Doebeli et al. 2005). Although as yet undiscovered ecological and reproductive traits may also have contributed to their sympatric divergence, it is likely that resource partitioning is not automatically coupled

with assortative mating. The only possible exception is that the difference in feeding sites between *O. nigrimas* and *O. nebulosus* led to a “mate-where-you-eat” preference (Via, 1999; Berlocher and Feder 2002; Forbes et al. 2009; Hadid et al. 2013, 2014). However, no such automatic magic trait is evident between *O. nigrimas*, and *O. orthognathus* or between *O. nebulosus*, and *O. orthognathus*. To understand how the sympatric speciation in this lake has been achieved without magic traits is challenging work in the field of studies of sympatric speciation.

CHAPTER 4

GENERAL DISCUSSION

4.1 How has sympatric speciation been completed without magic traits?

Empirical studies demonstrating sympatric speciation are rare (Bolnick and Fitzpatrick 2007 for review). Some consider that this is due not to its rarity, but because of the difficulty of empirically demonstrating this mode of speciation (e.g., Bird et al. 2012). In this study, I demonstrated that the three *Oryzias* species in Lake Poso have diverged in sympatry by testing the four criteria for sympatric speciation (Coyne and Orr 2004), i.e., (i) sympatric contemporary distributions, (ii) substantial reproductive isolation, (iii) phylogenetic sister relationships, and (iv) no historic phase of geographic isolation.

I also found that the three Poso species differ in resource utilization (Fig. 28A), and that assortative mating is well established (Fig. 28B), both of which are considered to be necessary for sympatric speciation to complete (Felsenstein 1981; Dieckmann and Doebeli 1999; Kondrashov and Kondrashov 1999; Doebeli et al. 2005). However, no apparent automatic magic trait was present among the three species, that is, the resource partitioning was not automatically coupled with assortative mating. This is especially true for the divergence between *O. nebulosus* and *O. orthognathus*. As mentioned above (Fig. 3), theories predict that sympatric speciation is difficult to complete without a magic trait, because recombination would erode the coupling between the ecological traits that allow resource partitioning and the reproductive traits that allow assortative mating (Dieckmann and Doebeli 1999; Kondrashov and Kondrashov 1999; Doebeli et al. 2005; Kopp et al. 2018).

Indeed, “magic traits” are known to be involved in most of the compelling examples of sympatric speciation. For example, in the case of *Rhagoletis* fruit flies, the utilization of fruits of different species automatically leads to spatial reproductive isolation between two

species (e.g., Feder and Busi 1989; Feder et al. 1998). The two fly species prefer different host plant species as a divergent response to fruit odors and oviposit on the fruits of the preferred plant. Therefore, the host plant preference is considered to be an automatic magic trait in the fruit flies. Similarly, in the case of sympatric speciation in the cichlids of African lakes, adaptation to different depths involve the evolution of light-sensing proteins that result in differential visual senses, which is an automatic magic trait that makes them reproductively isolated by the divergent use of microhabitats (Seehausen et al. 2008). Such traits that are related to “mate-where-you-eat” preference are typical automatic traits in most cases of the sympatric speciation that lead to spatial reproductive isolation. In the case of palm trees on an oceanic island, on the other hand, adaptation to different soil types induces the divergence of flowering times, which is another type of automatic magic trait that lead to temporal reproductive isolation (Savolainen et al. 2006). Martin (2013) and Martin et al. (2015) proposed that the evolution of automatic magic traits is likely to be a requirement for the completion of sympatric speciation.

Nevertheless, how have *O. nebulosus* and *O. orthognathus* diverged in sympatry without such automatic magic traits? I consider that oligotrophy of Lake Poso has played an important role in the disruptive selection of these three species. This lake is filled with very clear water (Giesen, 1994; Rintelen et al. 2012), with only very sparse periphyton on substrates (Fig. 25). This low-productivity ecosystem should impose strong disruptive selection on the feeding-related traits of diverging populations, because hybrid individuals might not exploit the food resources if they have suboptimal feeding morphologies (Fig. 29). The importance of such a postzygotic barrier in sympatric speciation recently been suggested among cichlids in a Nicaraguan crater lake, where sympatric speciation was also achieved without magic traits (Kautt et al. 2020).

Thus, the three *Oryzias* species in Lake Poso may have undergone sympatric speciation independently of automatic magic traits. Assuming that the common ancestor of the three Poso *Oryzias* had a short digestive tract, as in other Sulawesian adrianichthyids (Kakioka et al., unpublished), the evolution of long digestive tracts would have occurred twice: once in *O. nigrimas* and once in *O. nebulosus*. Alternatively, a long digestive tract would have evolved once in the common ancestor of the three species, followed by the re-evolution of a short digestive tract in *O. orthognathus*. However, the number of evolutionary events could be one if alleles for a short digestive tract were introgressed from an outgroup(s). In fact, ancient introgression from *O. soerotoi* to the common ancestor of *O. nebulosus* and *O. orthognathus* shortly before their divergence has been suggested from demographic inference based on genome-wide SNPs (analyses performed by Dr. J. Kusumi). Although the phenotypic consequences of introgressed genomic regions remain unclear, we infer that the completion of sympatric speciation may be possible even without automatic magic traits only if genetic variants that have diverged in allopatry are introgressed.

4.2 A new model system for the study on sympatric speciation

Ricefishes of the genus *Oryzias*, also known as medaka, are famous model organisms in the fields of genetics and developmental biology (e.g., Wittbrodt et al. 2002; Naruse et al.2011). Although the case studies of African and Nicaraguan cichlids have already secured their place as model systems for the study of sympatric speciation in fishes (e.g., Schliwen et al. 1994; Barluenga et al. 2006). This study indicates that ricefishes in this tectonic lake on a Wallacean island also have very high potential as a new model system for the study of sympatric speciation in the wild.

Especially, the ricefishes in Lake Poso may have a higher potential as a model system than others, because their sympatric speciation has been likely completed without magic traits.

As above, mechanisms of postzygotic isolation and the role of introgressive hybridization with another species outside the lake may be keys to solve solving this puzzle. For example, it will be essential to test the presence or absence of fitness decrease of hybrid individuals, i.e., if hybrid individuals can or cannot utilize the foods for their parental species, using laboratory experiments. It will be also important to identify the introgressed genomic regions and to examine their functions on reproductive isolation, using functional genomics approaches (such as in Kautt et al. 2020). They will be clarified in the near future using knowledge of this fish as a model organism for research in various fields of biology.

REFERENCES

Abendanon, E. C. 1915. Midden-Celebes-Expeditie. Geologische en geographische doorkruisingen van Midden-Celebes (1909–1910), Atlas. E. J. Brill, Leiden, The Netherlands.

Alexander, D. H., J. Novembre, and K. Lange. 2009. Fast model-based estimation of ancestry in unrelated individuals. Genome Res. 19:1655–1664.

Ansai, S., Mochida, K., Fujimoto, S., Mokodongan, D. F., Sumarto, B. K. A., Masengi, K. W. A., Hadiaty, R. K., Nagano A. J., Toyoda A., Naruse K., Yamahira. K., & Kitano, J. (2021). Genome editing reveals fitness effects of *Colony stimulating factor 1*, a gene responsible for diversification of sexual dichromatism in Sulawesian fishes. *Nature Communications*

Barluenga, M., K. N. Stölting, W. Salzburger, M. Muschick, and A. Meyer. 2006. Sympatric speciation in Nicaraguan crater lake cichlid fish. Nature 439:719–723.

Bird, C. E., I. Fernandez-Silva, D. J. Skillings, and R. J. Toonen. 2012. Sympatric speciation in the post "modern synthesis" era of evolutionary biology. Evol. Biol. 39:158–180.

Berlocher, S. H., & Feder, J. L. (2002). Sympatric speciation in phytophagous insects: moving beyond controversy? *Annual Review of Entomology*, 47, 773–815.

Blake, R.W. (1983). *Fish Locomotion*. Cambridge, UK: Cambridge University Press.

Bolnick, D. I., & Fitzpatrick, B. M. (2007). Sympatric speciation: Models and empirical evidence. *Annual Review of Ecology, Evolution, and Systematics*, 38, 459–487.

Bolger, A. M., M. Lohse, and B. Usadel. 2014. Trimmomatic: a flexible trimmer for Illumina sequence data. Bioinformatics 30:2114–2120.

Bolnick, D. I., and B. M. Fitzpatrick. 2007. Sympatric speciation: Models and empirical evidence. Annu. Rev. Ecol. Evol. Syst. 38:459–487.

Bouckaert, R. R. 2010. DensiTree: making sense of sets of phylogenetic trees. Bioinformatics 26:1372–1373.

Bouckaert, R., J. Heled, D. Kuhnert, T. Vaughan, C. H. Wu, D. Xie, M. A. Suchard, A. Rambaut, and A. J. Drummond. 2014. BEAST 2: a software platform for Bayesian evolutionary analysis. PLoS Comput. Biol. 10:e1003537.

Bryant, D., R. Bouckaert, J. Felsenstein, N. A. Rosenberg, and A. RoyChoudhury. 2012. Inferring species trees directly from biallelic genetic markers: bypassing gene trees in a full coalescent analysis. Mol. Biol. Evol. 29:1917–1932.

Catchen, J. M., A. Amores, P. A. Hohenlohe, W. A. Cresko, and J. Postlethwait. 2011. Stacks: building and genotyping loci de novo from short-read sequences. G3-Genes Genom. Genet. 1:171–182.

Catchen, J., P. A. Hohenlohe, S. Bassham, A. Amores, and W. A. Cresko. 2013. Stacks: an analysis tool set for population genomics. Mol. Ecol. 22:3124–3140.

Coyne, J. A., and H. A. Orr. 2004. Speciation. Sinauer Associates, Sunderland, MA.

Danecek, P., A. Auton, G. Abecasis, C. A. Albers, E. Banks, M. A. DePristo, R. E. Handsaker, G. Lunter, G. T. Marth, S. T. Sherry, G. McVean, R. Durbin, and 1000 Genomes Project Analysis Group. 2011. The variant call format and VCFtools. Bioinformatics 27:2156–2158.

Darriba, D., G. L. Taboada, R. Doallo, and D. Posada. 2012. JModelTest 2: more models, new heuristics and parallel computing. Nat. Methods 9:772.

Dieckmann, U., and M. Doebeli. 1999. On the origin of species by sympatric speciation. Nature 400:354–357.

Doebeli, M., Dieckmann, U., Metz, J. A. J., & Tautz, D. (2005). What we have also learned: adaptive speciation is theoretically plausible. Evolution, 59, 691–695.

Echelle, A. A., E. W. Carson, A. F. Echelle, R. A. Van Den Bussche, T. E. Dowling, and A. Meyer. 2005. Historical biogeography of the New-World pupfish genus *Cyprinodon* (Teleostei: Cyprinodontidae). Copeia 2005:320–339.

Excoffier, L., and H. E. L. Lischer. 2010. Arlequin suite ver 3.5: a new series of programs to perform population genetics analyses under Linux and Windows. Mol. Ecol. Resour. 10:564–567.

Excoffier, L., I. Dupanloup, E. Huerta-Sánchez, V. C. Sousa, and M. Foll. 2013. Robust demographic inference from genomic and SNP data. PLOS Genetics, 9(10):e1003905.

Feder J.L., Bush G.L. 1989. A field test of differential host-plant usage between two sibling species of *Rhagoletis pomonella* fruit flies (Diptera: Tephritidae) and its consequences for sympatric models of speciation. Evolution, 43: 1813–1819.

Feder J.L., Berlocher S.H., Opp S.B. 1998. Sympatric host-race formation and speciation in *Rhagoletis* (Diptera: Tephritidae): A tale of two species for Charles D. In: S. Mopper, S. Y. Strauss eds. *Genetic Structure and Local Adaptation in Natural Insect Populations*, (pp. 408–441). Dordrecht: Springer.

Felsenstein, J. (1981). Skepticism towards Santa Rosalia, or why are there so few kinds of animals? Evolution, 35:124–138.

Foote, A. D. 2018. Sympatric speciation in the genomic era. Trends Ecol. Evol. 33:85–95.

Forbes, A. A., Powell, T. H. Q., Stelinski, L. L., Smith, J. J., & Feder, J. L. (2009). Sequential sympatric speciation across trophic levels. *Science*, 323, 776–779.

Futuyma, D. J., & Mayer, G. C. (1980). Non-allopatric speciation in animals. *Systematic Zoology*, 29, 254–271.

German, D. P. (2011). Digestive Efficiency. In: A. P. Farrell (Ed.), *Encyclopedia of Fish Physiology: From Genome to Environment, Volume 3* (pp. 1596–1607). San Diego, CA: Academic Press.

Giesen, W. (1994). Indonesia's major freshwater lakes: a review of current knowledge, development processes and threats. *Internationale Vereinigung für Theoretische und Angewandte Limnologie*, 24, 115–128.

Guo, B. C., F. J. J. Chain, E. Bornberg-Bauer, E. H. Leder, and J. Merila. 2013. Genomic divergence between nine- and three-spined sticklebacks. BMC Genomics 2013:14.

Hadid, Y., Tzur, S., Pavlíček, T., Šumbera, R., Šklíba, J., Lövy, M., Fragman-Sapir, O., Beiles, A., Arieli, R., Raz, S., & Nevo, E. (2013). Possible incipient sympatric ecological speciation in blindmole rats (*Spalax*). *Proceedings of the National Academy of Science of the United States of America*, 110, 2587–2592.

Hadid, Y., Pavlíček, T., Beiles, A., Ianovici, R., Raz, S., & Nevo, E. (2014). Sympatric incipient speciation of spiny mice *Acomys* at "Evolution Canyon," Israel. *Proceedings of the National Academy of Science of the United States of America*, 111, 1043–1048.

Harada, S., S. R. Joen, I. Kinoshita, M. Tanaka, and M. Nishida. 2002. Phylogenetic relationships of four species of floating gobies (*Gymnogobius*) as inferred from partial mitochondrial cytochrome *b* gene sequences. Ichtyol. Res. 49:324–332.

Herder, F., R. K. Hadiaty, and A. W. Nolte. 2012. Pelvic-fin brooding in a new species of riverine ricefish (Atherinomorpha: Beloniformes: Adrianichthyidae) from Tana Toraja, Central Sulawesi, Indonesia. Raffles Bull. Zool. 60:467–476.

Herder, F., A. W. Nolte, J. Pfaender, J. Schwarzer, R. K. Hadiaty, and U. K. Schliewen. 2006. Adaptive radiation and hybridization in Wallace's Dreamponds: evidence from sailfin silversides in the Malili Lakes of Sulawesi. Proc. R. Soc. B Biol. Sci. 273:2209–2217.

Herder, F., J. Pfaender, and U. K. Schliewen. 2008. Adaptive sympatric speciation of polychromatic "roundfin" sailfin silverside fish in Lake Matano (Sulawesi). Evolution 62:2178–2195.

Higashi, M., G. Takimoto, and N. Yamamura. 1999. Sympatric speciation by sexual selection. Nature 402:523–526.

Huson, D. H., and D. Bryant. 2006. Application of phylogenetic networks in evolutionary studies. Mol. Biol. Evol. 23:254–267.

Iwamatsu, T. (2006). *The Integrated Book for the Biology of the Medaka.* Okayama, Japan: Daigaku Kyouiku Publications (in Japanese).

Jombart, T. (2008). *adegenet*: a R package for the multivariate analysis of genetic markers. *Bioinformatics*, 24, 1403–1405.

Jombart, T., & Ahmed, I. (2011). adegenet 1.3-1: new tools for the analysis of genome-wide SNP data. *Bioinformatics*, 27, 3070–3071.

Joyce, D. A., D. H. Lunt, M. J. Genner, G. F. Turner, R. Bills, and O. Seehausen. 2011. Repeated colonization and hybridization in Lake Malawi cichlids. Curr. Biol. 21:R108–R109.

Kautt, A. F., G. Machado-Schiaffino, and A. Meyer. 2016. Multispecies outcomes of sympatric speciation after admixture with the source population in two radiations of Nicaraguan crater lake cichlids. PLoS Genet. 12:e1006157.

Kondrashov, A. S., and F. A. Kondrashov. 1999. Interactions among quantitative traits in the course of sympatric speciation. Nature 400:351–354.

Kopelman, N. M., Mayzel, J., Jakobsson, M., Rosenberg, N. A., & Mayrose, I. (2015). CLUMPAK: a program for identifying clustering modes and packaging population structure inferences across *K*. *Molecular Ecology Resources*, 15, 1179–1191.

Kopp, M., Servedio, M. R., Mendelson, T. C., Safran, R. J., Rodríguez, R. L., Hauber, M. E., Scordato, E. C., Symes, L. B., Balakrishnan, C. N., Zonana, D. M., & van Doorn, G. S. (2018). Mechanisms of assortative mating in speciation with gene flow: connecting theory and empirical research. *The American Naturalist*, *191*, 1–20.

Kottelat, M. 1990. Synopsis of the endangered buntingi (Osteichthyes: Adrianichthyidae and Oryziidae) of Lake Poso, Central Sulawesi, Indonesia, with a new reproductive guild and descriptions of three new species. Ichthyol. Explor. Freshwaters 1:49–67.

Klingenberg, C. P. (2011). MorphoJ: an integrated software package for geometric morphometrics. *Molecular Ecology Resources*, 11, 353–357.

Kumar, S., G. Stecher, and K. Tamura. 2016. MEGA7: molecular evolutionary genetics analysis version 7.0 for bigger datasets. Mol. Biol. Evol. 33:1870–1874.

Kutschera, V. E., T. Bidon, F. Hailer, J. L. Rodi, S. R. Fain, and A. Janke. 2014. Bears in a forest of gene trees: phylogenetic inference is complicated by incomplete lineage sorting and gene flow. Mol. Biol. Evol. 31:2004–2017.

Langerhans, R. B., & Reznick, D. N. (2010). Ecology and evolution of swimming performance in fishes: predicting evolution with biomechanics. In P. Domenici & B. G. Kapoor (Eds.), *Fish Locomotion: An Eco-Ethological Perspective* (pp. 200–248). Enfield, London: Science Publishers.

Li, H. (2011). A statistical framework for SNP calling, mutation discovery, association mapping and population genetical parameter estimation from sequencing data. *Bioinformatics*, 27, 2987–2993.

Librado, P., and J. Rozas. 2009. DnaSP v5: a software for comprehensive analysis of DNA polymorphism data. Bioinformatics 25:1451–1452.

Lunter, G., and M. Goodson. 2011. Stampy: a statistical algorithm for sensitive and fast mapping of Illumina sequence reads. Genome Res. 21:936–939.

Maddison, W. P. 1997. Gene trees in species trees. Syst. Biol. 46:523–536.

Malinsky, M., H. Svardal, A. M. Tyers, E. A. Miska, M. J. Genner, G. F. Turner, and R. Durbin. 2018. Whole-genome sequences of Malawi cichlids reveal multiple radiations interconnected by gene flow. Nature Ecol. Evol. 2:1940–1955.

Mandagi, I. F., D. F. Mokodongan, R. Tanaka, and K. Yamahira. 2018 A new riverine ricefish of the genus *Oryzias* (Beloniformes, Adrianichthyidae) from Malili, central Sulawesi, Indonesia. Copeia 106:297–304.

Marques, D. A., J. I. Meier, and O. Seehausen. 2019. A combination view on speciation and adaptive radiation. Trends Ecol. Evol. 34:531–544.

Martin, C. H. 2012. Weak disruptive selection and incomplete phenotypic divergence in two classic examples of sympatric speciation: Cameroon crater lake cichlids. Am. Nat. 180:E90–E109.

Martin, C. H. 2013. Strong assortative mating by diet, color, size, and morphology but limited progress toward sympatric speciation in a classic example: Cameroon crater lake cichlids. Evolution 67:2114–2123.

Martin, C. H., J. S. Cutler, J. P. Friel, C. D. Touokong, G. Coop, and P. C. Wainwright. 2015. Complex histories of repeated gene flow in Cameroon crater lake cichlids cast doubt on one of the clearest examples of sympatric speciation. Evolution 69:1406–1422.

Martin, C. H., and L. C. Feinstein. 2014. Novel trophic niches drive variable progress towards ecological speciation within an adaptive radiation of pupfishes. Mol. Ecol. 23:1846–1862.

Mayr, E. (1963). *Animal Species and Evolution*. Cambridge, MA: Belknap.

Mayr, E. 1992. Darwin's principle of divergence. J. Hist. Biol. 25:343–359.

McCann, K. S., Rasmussen, J. B. & Umbanhowar, J. (2005). The dynamics of spatially coupled food webs. *Ecology Letters*, 8, 513–523.

Meier, J. I., D. A. Marques, S. Mwaiko, C. E. Wagner, L. Excoffier, and O. Seehausen. 2017. Ancient hybridization fuels rapid cichlid fish adaptive radiations. Nat. Commun. 8:14363.

Mokodongan, D. F., R. Tanaka, and K. Yamahira. 2014. A new ricefish of the genus *Oryzias* (Beloniformes, Adrianichthyidae) from Lake Tiu, Central Sulawesi, Indonesia. Copeia 2014:561–567.

Mokodongan, D. F., and K. Yamahira. 2015a. Origin and intra-island diversification of Sulawesi endemic Adrianichthyidae. Mol. Phylogenet. Evol. 93:150–160.

Mokodongan, D. F., and K. Yamahira. 2015b. Mitochondrial and nuclear phylogenies and divergence time estimations of Sulawesi endemic Adrianichthyidae. Data in Brief 5:281–284.

Mokodongan, D. F., Montenegro, J., Mochida, K., Fujimotoa, S., Ishikawa, A., Kakioka, R., Yong, L., Mulis, Hadiaty, R. K., Mandagi, I. F., Masengi, K. W.A., Wachi, N., Hashiguchi, Y., Kitano, J., & Yamahira, K. (2018). Phylogenomics reveals habitat-associated body shape divergence in *Oryzias woworae* species group (Teleostei: Adrianichthyidae). *Molecular Phylogenetics and Evolution*, 118, 194–203.

Naruse, K., M. Tanaka, and H. Takeda. 2011. Medaka: A model for organogenesis, human disease, and evolution. Springer, Tokyo, Japan.

Nei, M. 1972. Genetic distance between populations. Am. Nat. 106:283–292.

Nichols, R. 2001. Gene trees and species trees are not the same. Trends Ecol. Evol. 16:358–364.

Orti, G., M. A. Bell, T. E. Reimchen, and A. Meyer. 1994. Global survey of mitochondrial DNA sequences in the threespine stickleback: evidence for recent migrations. Evolution 48:608–622.

Parenti, L. R. 2008. A phylogenetic analyses and taxonomic revision of ricefishes, *Oryzias* and relatives (Beloniformes, Adrianichthyidae). Zool. J. Linn. Soc. 154:494–610.

Parenti, L. R., and B. Soeroto. 2004. *Adrianichthys roseni* and *Oryzias nebulosus*, two new ricefishes (Atherinomorpha: Beloniformes: Adrianichthyidae) from Lake Poso, Sulawesi, Indonesia. Ichthyol. Res. 51:10–19.

Pembleton, L. W., N. O. I. Cogan, and J. W. Foster. 2013. StAMPP: an R package for calculation of genetic differentiation and structure of mixed-ploidy level populations. Mol. Ecol. 13:946–952.

Peterson, B. B. K., J. N. J. Weber, E. H. E. Kay, H. S. Fisher, and H. E. Hoekstra. 2012. Double digest radseq: an inexpensive method for de novo SNP discovery and genotyping in model and non-model species. PLoS One 7:e37135.

Pfeifer B., U. Wittelsbürger, S. E. Ramos-Onsins, and M .J. Lercher. 2014. PopGenome: an efficient Swiss army knife for population genomic analyses in R. Mol. Biol. Evol. 31:1929–1936.

Pfennig, D. W., and K. S. Pfennig. 2012. Evolution's wedge: competition and the origins of diversity. Univ. of California Press, Berkeley, CA.

Pickrell, J. K., and J. K. Pritchard. 2012. Inference of population splits and mixtures from genome-wide allele frequency data. PLoS Genet. 8:e1002967.

Purcell, S., B. Neale, K. Todd-Brown, L. Thomas, M. A. R. Ferreira, D. Bender, J. Maller, P. Sklar, P. I. W. de Bakker, M. J. Daly, and P. C. Sham. 2007. PLINK: a tool set for whole-genome association and population-based linkage analyses. Am. J. Hum. Genet. 81:559–575.

Rambaut, A., M. A. Suchard, D. Xie, and A. J. Drummond. 2014. Tracer v1.6. Available from http://beast.bio.ed.ac.uk/Tracer.

R Core Team (2020). *R: A Language and Environment for Statistical Computing*. Vienna: R Foundation for Statistical Computing.

R Development Core Team. 2014. R: A language and environment for statistical computing. R Foundation for Statistical Computing, Vienna, Austria, URL http://www.R-project.org/.

Reich, D., K. Thangaraj, N. Patterson, A. L. Price, and L. Singh. 2009. Reconstructing Indian population history. Nature 461:489–494.

Richards, E. J., M. R. Servedio, and C. H. Martin. 2019. Searching for sympatric speciation in the genomic era. BioEssays 41:1900047.

Rochette, N.C., Rivera-Colón, A. G., Catchen, J. M. (2019). Stacks 2: Analytical methods for paired-end sequencing improve RADseq-based population genomics. *Molecular Ecology*, 28, 4737–4754.

Sakaguchi, S., T. Sugino, Y. Tsumura, M. Ito, M. D. Crisp, D. M. J. S. Bowman, A. J. Nagano, M. N. Honjo, M. Yasugi, H. Kudoh, Y. Matsuki, Y. Suyama, and Y. Isagi. 2015. High-throughput linkage mapping of Australian white cypress pine (*Callitris glaucophylla*) and map transferability to related species. Tree Genet. Genomes 11:121.

Savolainen, V., M.-C. Anstett, C. Lexer, I. Hutton, J. J. Clarkson, M. V. Norup, M. P. Powell, D. Springate, N. Salamin, and W. J. Baker. 2006. Sympatric speciation in palms on an oceanic island. Nature 441:210–213.

Schliewen, U. K., D. Tautz, and S. Paabo. 1994. Sympatric speciation suggested by monophyly of crater lake cichlids. Nature 368:629–632.

Servedio, M. R., van Doorn, G. S., Kopp, M., Frame, A. M., & Nosil, P. (2011). Magic traits in speciation: “magic” but not rare? *Trends in Ecology & Evolution*, 26, 389–397.

Seehausen, O. 2004. Hybridization and adaptive radiation. Trends Ecol. Evol. 19:198–207.

Seehausen O., Terai Y., Magalhaes I.S., Carleton K.L., Mrosso H.D., Miyagi R., van der Sluijs I., Schneider M.V., Maan M.E., Tachida H., Imai H., Okada N. 2008. Speciation through sensory drive in cichlid fish. Nature, 455: 620–626.

Silvestro, D., and I. Michalak. 2012. RaxmlGUI: a graphical front-end for RAxML. Org. Divers. Evol. 12:335–337.

Sorenson, M. D., K. M. Sefc, and R. B. Payne. 2003. Speciation by host switch in brood parasitic indigobirds. Nature 424:928–931.

Stelbrink, B., C. Albrecht, R. Hall, and T. von Rintelen. 2012. The biogeography of Sulawesi revisited: is there evidence for a vicariant origin of taxa on Wallace's "anomalous island"? Evolution 66:2252–2271.

Sutra, N., Kusumi, J., Montenegro, J., Kobayashi, H., Fujimoto, S., Masengi, K. W. A., Nagano, A. J., Toyoda, A., Matsunami, M., Kimura, R., & Yamahira, K. (2019). Evidence for sympatric speciation in a Wallacean ancient lake. Evolution, 73, 1898–1915.

Takehana, Y., N. Nagai, M. Matsuda, K. Tsuchiya, and M. Sakaizumi. 2003. Geographic variation and diversity of the cytochrome b gene in Japanese wild populations of medaka, *Oryzias latipes*. Zool. Sci. 20:1279–1291.

Takehana, Y., K. Naruse, and M. Sakaizumi. 2005. Molecular phylogeny of the medaka fishes genus *Oryzias* (Beloniformes: Adrianichthyidae) based on nuclear and mitochondrial DNA sequences. Mol. Phylogenet. Evol. 36:417–428.

Tayasu, I., Hirasawa, R., Ogawa, N. O., Ohkouchi, N., & Yamada, K. (2011). New organic reference materials for carbon- and nitrogen-stable isotope ratio measurements provided by Center for Ecological Research, Kyoto University, and Institute of Biogeosciences, Japan Agency for Marine-Earth Science and Technology. *Limnology*, 12, 261–266.

Turelli, M., N. H. Barton, and J. A. Coyne. 2001. Theory and speciation. Trends Ecol. Evol. 16:330–343.

Via, S. (1999). Reproductive isolation between sympatric races of pea aphids. I. Gene flow restriction and habitat choice. *Evolution*, 53, 1446–1457.

von Rintelen, T., and M. Glaubrecht. 2006. Rapid evolution of sessility in an endemic species flock of the freshwater bivalve *Corbicula* from ancient lakes on Sulawesi, Indonesia. Biol. Lett. 2:73–77.

von Rintelen, K., M. Glaubrecht, C. D. Schubart, A. Wessel, and T. von Rintelen. 2010. Adaptive radiation and ecological diversification of Sulawesi's ancient lake shrimps. Evolution 64:3287–3299.

von Rintelen, K., T. von Rintelen, and M. Glaubrecht. 2007. Molecular phylogeny and diversification of freshwater shrimps (Decapoda, Atyidae, *Caridina*) from ancient Lake Poso (Sulawesi, Indonesia) – the importance of being colourful. Mol. Phylogenet. Evol. 45:1033–1041.

von Rintelen, T., K. von Rintelen, M. Glaubrecht, C. D. Schubart, and F. Herder. 2012. Aquatic biodiversity hotspots in Wallacea: the species flocks in the ancient lakes of Sulawesi, Indonesia. Pp. 290–315 in D. J. Gower, K. G. Johnson, J. E. Richardson, B. R. Rosen, L. Rüber, S. T. Williams, eds. Biotic evolution and environmental change in southeast Asia. Cambridge Univ. Press, Cambridge.

von Rintelen, T., A. B. Wilson, A. Meyer, and M. Glaubrecht. 2004. Escalation and trophic specialization drive adaptive radiation of viviparous freshwater gastropods in the ancient lakes on Sulawesi, Indonesia. Proc. R. Soc. B 271:2541–2549.

Webb, P. W. (1984). Body form, locomotion and foraging in aquatic vertebrates. *American Zoologist*, 24, 107–120.

Wigginton, J. E., D. J. Cutler, and G. R. Abecasis. 2005. A note on exact tests of Hardy-Weinberg equilibrium. Am. J. Hum. Genet. 76:887–893.

Wittbrodt, J. A. Shima, and M. Scharti. 2002. Medaka – A model organism from the Far East. Nat. Rev. Genet. 3:53–64.

Wootton, R. J. (1998). *Ecology of Teleost Fishes, second edition*. Dordrecht, The Netherlands: Kluwer Academic Publishers.

Zheng X., D. Levine, J. Shen, S. M. Gogarten, C. Laurie, and B. S. Weir. 2012. A high-performance computing toolset for relatedness and principal component analysis of SNP data. Bioinformatics 28:3326–3328.

Zhou, Y., L. Duvaux, G. Ren, L. Zhang, O. Savolainen, and J. Liu. 2017. Importance of incomplete lineage sorting and introgression in the origin of shared genetic variation between two closely related pines with overlapping distributions. Heredity 118:211–220.

Table 1. Substitution models used in the BEAST analyses.

Gene	1st codon	2nd codon	3rd codon
ND2	HKY+G	GTR+I	GTR
cyt *b*	TN93	TN93	GTR+G

Table 2. Results of ANOVA of the effects of standard length, species, sex, and their interactions on body depth.

Source of variation	df	MS	*F* value	*P*
Standard length	1	122.262	868.222	< 0.0001
Species	2	6.462	45.887	< 0.0001
Sex	1	0.487	3.456	0.0685
Standard length × Species	2	0.858	6.094	0.0041
Standard length × Sex	1	0.758	5.386	0.0241
Species × Sex	2	0.049	0.349	0.7073
Standard length × Species × Sex	2	0.061	0.432	0.6515
Residuals	54	0.141		

Table 3. Frequency distributions for (A) the number of scales along the lateral midline, (B) the number of pectoral-fin rays, (C) the number of anal-fin rays, and (D) the number of vertebrae, for the three *Oryzias* species endemic to Lake Poso. Numbers in parentheses indicate the number of males.

(A) Lateral scale	33	34	35	36	37	⋯	52	53	54
O. nigrimas	–	–	–	13(6)	6(2)	–	–	–	–
O. nebulosus	3(1)	11(8)	13(10)	–	–	–	–	–	–
O. orthognathus	–	–	–	–	–	–	2(0)	7(3)	11(8)

(B) Pectoral fin ray	9	10	11	12
O. nigrimas	–	15(6)	4(2)	–
O. nebulosus	1(1)	26(18)	–	–
O. orthognathus	–	–	18(11)	2(0)

(C) Anal fin ray	20	21	22	23	24	25
O. nigrimas	–	1(1)	5(4)	6(2)	6(1)	1(0)
O. nebulosus	2(0)	11(9)	8(6)	6(4)	–	–
O. orthognathus	–	–	3(1)	11(5)	6(5)	–

(A) Vertebrae	30	31	32	33	34	35
O. nigrimas	–	–	–	6(1)	12(6)	1(1)
O. nebulosus	1(0)	10(7)	15(11)	1(1)	–	–
O. orthognathus	–	–	10(5)	10(6)	–	–

Table 4. Results of ANOVA of the effects of species, sex, and their interaction on (A) PC1 and (B) PC2.

(A) PC1

Source of variation	df	MS	*F* value	*P*
Species	2	64.440	227.3610	< 0.0001
Sex	1	0.010	0.0366	0.8489
Species × Sex	2	0.313	1.1051	0.3378
Residuals	60	0.283		

(B) PC2

Source of variation	df	MS	*F* value	*P*
Species	2	26.3973	86.3760	< 0.0001
Sex	1	0.6009	1.9664	0.1660
Species × Sex	2	0.3063	1.0022	0.3731
Residuals	60	0.3056		

Table 5. List of samples used in this study. PSA, population structure analyses; MA, morphological analyses; and SIA, stable isotope analyses.

Species	Collection site	N	Preservation	Application purpose	Collected year or reference
Oryzias nigrimas	Tentena	4	Ethanol	PSA	2018
	Tentena	20	Formalin	MA	2019
	Saluopa	16	Ethanol	PSA	Sutra et al. (2019)
	Taipa	5	Ethanol	PSA	2018
	Taipa	20	Ethanol	SIA	2018
	Pendolo	1	Ethanol	PSA	2018
	Peura	1	Ethanol	PSA	2018
Oryzias orthognathus	Tentena	2	Ethanol	PSA	2018
	Tentena	20	Formalin	MA	2019
	Saluopa	20	Ethanol	PSA	Sutra et al. (2019)
	Taipa	7	Ethanol	PSA	2018
	Taipa	20	Ethanol	SIA	2018
	Tolambo	10	Ethanol	PSA	2018
Oryzias nebulosus	Saluopa	7	Ethanol	PSA	Sutra et al. (2019)
	Taipa	8	Ethanol	PSA	2018
	Dumulanga	19	Ethanol	PSA	Sutra et al. (2019)
	Dumulanga	20	Formalin	MA	2019
	Dumulanga	20	Ethanol	SIA	2018
	Tolambo	5	Ethanol	PSA	2012

Table 6. Results of two-way analyses of variance of the effects of species and sex on (a) PC1 and (b) PC2 scores in the geometric morphometric analysis.

(a) PC1

Source of variation	df	SS	*F* value	*P*
Species	2	0.0193	108.3310	< 0.0001
Sex	1	0.0001	1.0404	0.3123
Species × Sex	2	0.0006	3.4656	0.0384
Residuals	54	0.0048		

(b) PC2

Source of variation	df	SS	*F* value	*P*
Species	2	0.0086	79.6282	< 0.0001
Sex	1	0.0000	0.0256	0.8735
Species × Sex	2	0.0009	8.3099	0.0007
Residuals	54	0.0029		

Table 7. Result of two-way analysis of covariance of the effects of standard length, species, and sex on digestive tract length.

Source of variation	df	SS	*F* value	*P*
Standard length	1	0.2375	13.5424	0.0005
Species	2	3.7432	106.7118	< 0.0001
Sex	1	0.0347	1.9796	0.1653
Species × Sex	2	0.0742	2.1148	0.1307
Residuals	53	0.9296		

Table 8. Result of two-way analysis of covariance of the effects of standard length, species, and sex on gill arch length.

Source of variation	df	SS	*F* value	*P*
Standard length	1	10.2239	18.2666	< 0.0001
Species	2	76.9646	68.7549	< 0.0001
Sex	1	0.03342	0.0597	0.8079
Species × Sex	2	5.3795	4.8056	0.0121
Residuals	53	29.6643		

Table 9. Result of two-way analysis of variance of the effects of species and sex on gill raker number.

Source of variation	df	SS	*F* value	*P*
Species	2	272.6333	79.8384	< 0.0001
Sex	1	1.6667	0.9761	0.3276
Species × Sex	2	6.4333	1.8839	0.1618
Residuals	54	92.2000		

Table 10. Results of two-way analyses of variance of the effects of species and sex on (a) gill raker length and (b) gill raker interval.

(a) Gill raker length

Source of variation	df	SS	*F* value	*P*
Species	2	6.0677	135.9487	< 0.0001
Raker position	13	8.3504	28.7833	< 0.0001
Species × Raker position	26	1.8434	3.1770	< 0.0001
Residuals	84	1.8746		

(b) Gill raker interval

Source of variation	df	SS	*F* value	*P*
Species	2	0.5451	30.7431	< 0.0001
Raker position	12	5.4492	51.2175	< 0.0001
Species × Raker position	24	0.6872	3.2296	< 0.0001
Residuals	78	0.6916		

Table 11. Results of two-way analysis of variance of the effects of species and sex on (a) $\delta^{13}C$ and (b) $\delta^{15}N$ values in the stable isotope analyses.

(a) $\delta^{13}C$

Source of variation	df	SS	*F* value	*P*
Species	2	224.9163	60.5896	< 0.0001
Sex	1	10.3339	5.5676	0.0219
Species × Sex	2	2.1830	0.5881	0.5589
Residuals	54	100.2274		

(b) $\delta^{15}N$

Source of variation	df	SS	*F* value	*P*
Species	2	4.2232	34.6755	< 0.0001
Sex	1	0.1652	2.7125	0.1054
Species × Sex	2	0.0532	0.4371	0.6482
Residuals	54	3.2884		

Table 12. Result of partially nested three-way analysis of variance of the effects of male species (conspecific versus heterospecific), female species, and female individual (nested within female species) on average time until spawning.

Source of variation	df	SS	*F* value	*P*
Male species	1	28532.8	61.6334	0.0014
Female species	1	31005.3	49.4656	0.0022
Male species × Female species	1	10285.3	22.2172	0.0092
Female (female species)	4	2507.2	1.3540	0.3881
Male species × Female (female species)	4	1851.8	0.9160	0.4707
Residuals	24	12129.7		

Table 13. Day of first spawning in each of the intra- and interspecific mating trials. Numbers indicate frequency of days upon which the first spawning occurred among the nine combinations of pairs (i.e., round robin among three females and three males).

Combination	Day of the first spawning		
	Day 1	Day 2	Day 3
O. nebulosus Female × *O. nebulosus* Male	8	1	0
O. nebulosus Female × *O. orthognathus* Male	0	4	5
O. orthognathus Female × *O. orthognathus* Male	6	3	0
O. orthognathus Female × *O. nebulosus* Male	0	4	5

Table 14. Color change sequences involved in mating behaviors. Numbers indicate frequency of each sequence among 27 observations of mating behaviors (i.e., three replicates of each of the nine combinations of pairs). MB: male became black; FB: female became black; and MW: male became whitish. Note that all females that became black spawned thereafter.

Color change sequences	*O. nebulosus* Males		*O. orthognathus* Male	
	× *O. nebulosus* Female	× *O. orthognathus* Female	× *O. orthognathus* Female	× *O. nebulosus* Female
No color change	0	0	16	16
MB	8	15	1	0
MB→FB	17	0	10	9
MB→MW	2	3	0	2
MB→MW→MB→FB	0	9	0	0

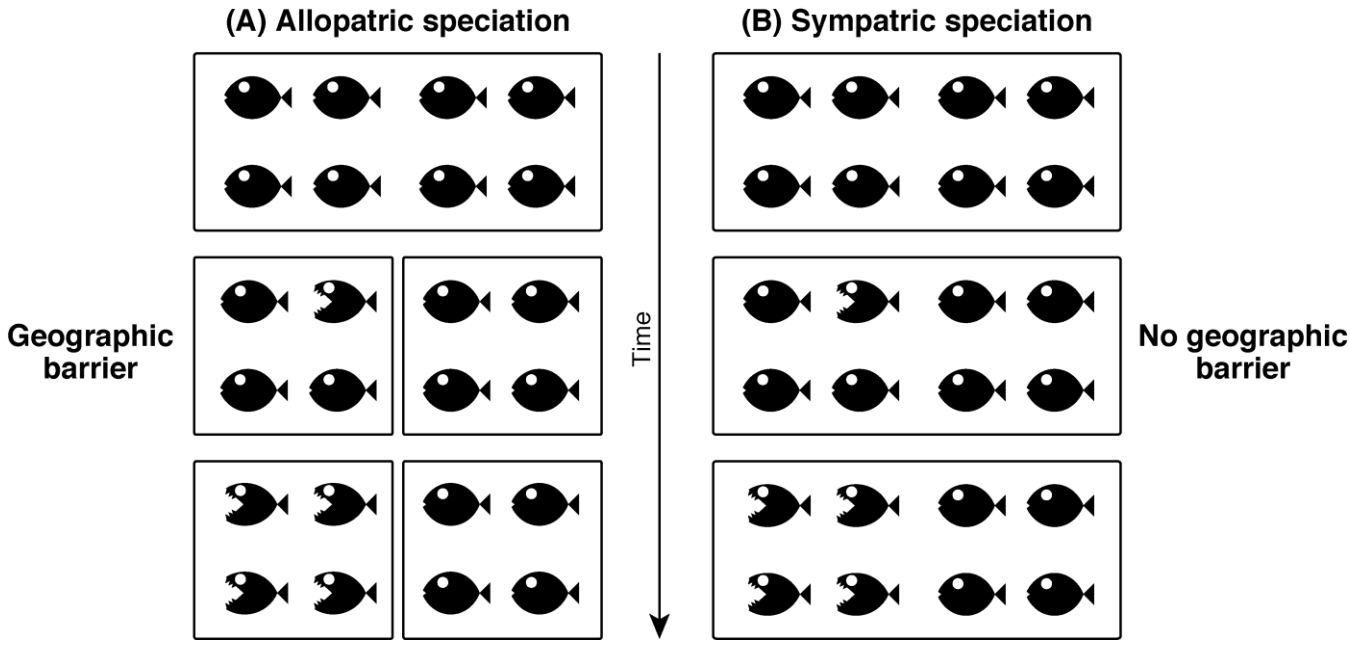

Figure 1. Schematic illustration of the process of (A) allopatric speciation and (B) sympatric speciation.

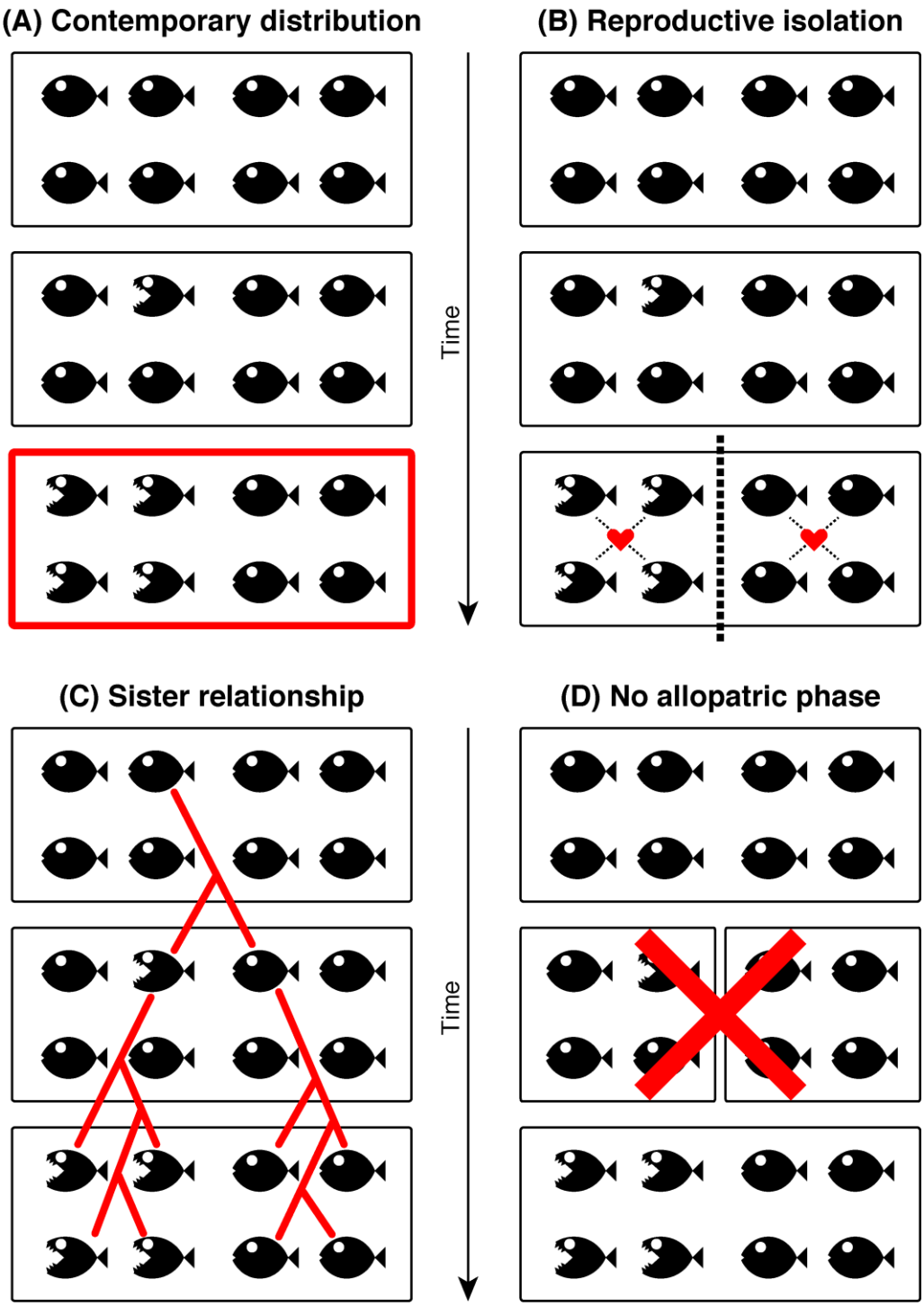

Figure 2. Schematic illustration of the four criteria by Coyne and Orr (2004) necessary to be satisfied to demonstrate sympatric speciation, i.e., (A) sympatric contemporary distributions, (B) genetically-based reproductive isolation, (C) phylogenetic sister relationships, and (D) no historic phase of geographic isolation.

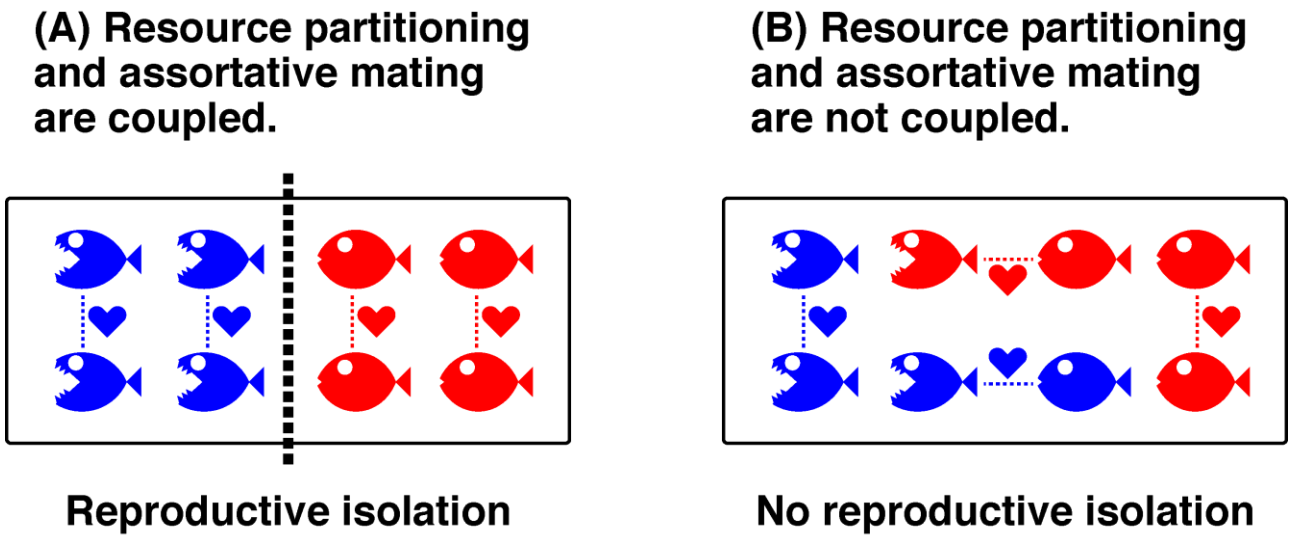

Figure 3. Schematic illustration to explain why resource partitioning must be coupled assortative mating for sympatric speciation to be completed. (A) If resource partitioning (shown as large vs. small mouths) and assortative mating (shown as red vs. blue colors) are coupled in some ways, i.e., if individuals with large (small) mouths are always blue (red), sympatric speciation will be completed. "Automatic magic traits", which allow populations not only to use different resources but also to mate assortatively as a byproduct of resource partitioning, would generate this situation. (B) If resource partitioning and assortative mating are not coupled, i.e., if some individuals with large (small) mouths are red (blue), sympatric speciation will not be completed, because individuals having different resource utilization will mate with each other.

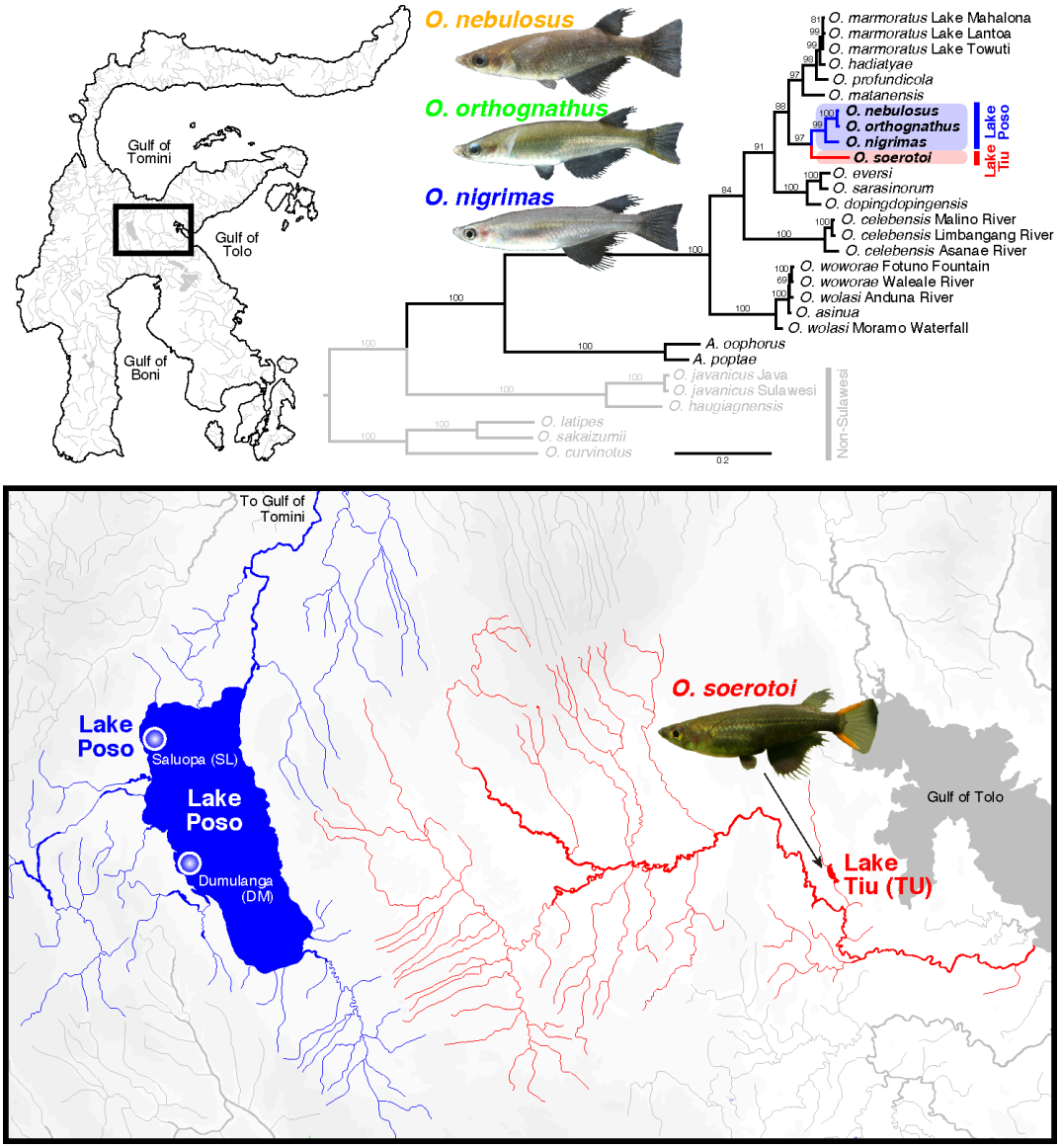

Figure 4. Maximum likelihood (ML) phylogeny of Sulawesi adrianichthyids based on mtDNA sequences (ND2: 1,053 bp; cyt *b*: 1,141 bp) and a map showing locations of the collection sites. The water systems of Lake Poso and Lake Tiu are indicated by blue and red, respectively. Map provided by Thomas von Rintelen and modified.

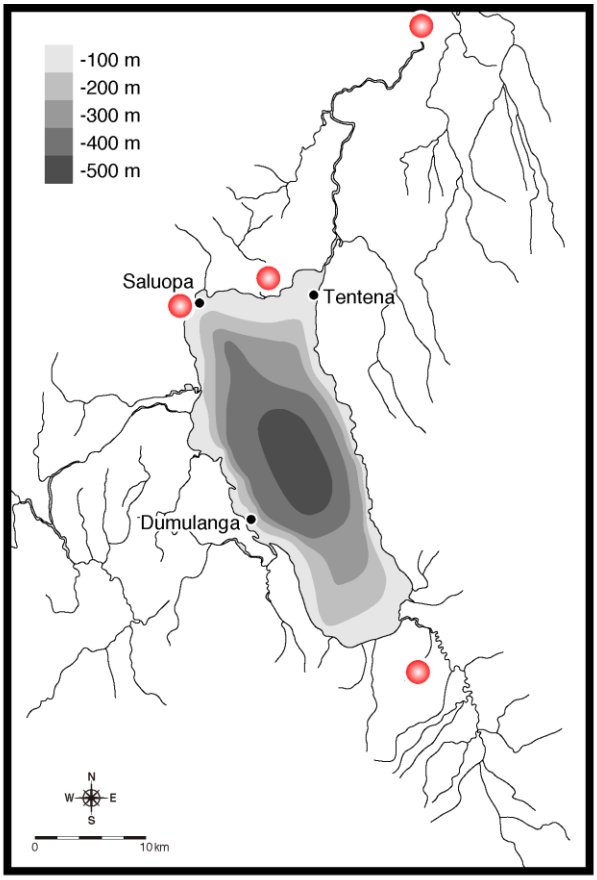

Figure 5. Bathymetry map of Lake Poso, showing locations of sites where riverine *Oryzias* were searched for. Map modified from Rintelen et al. (2012), with permission.

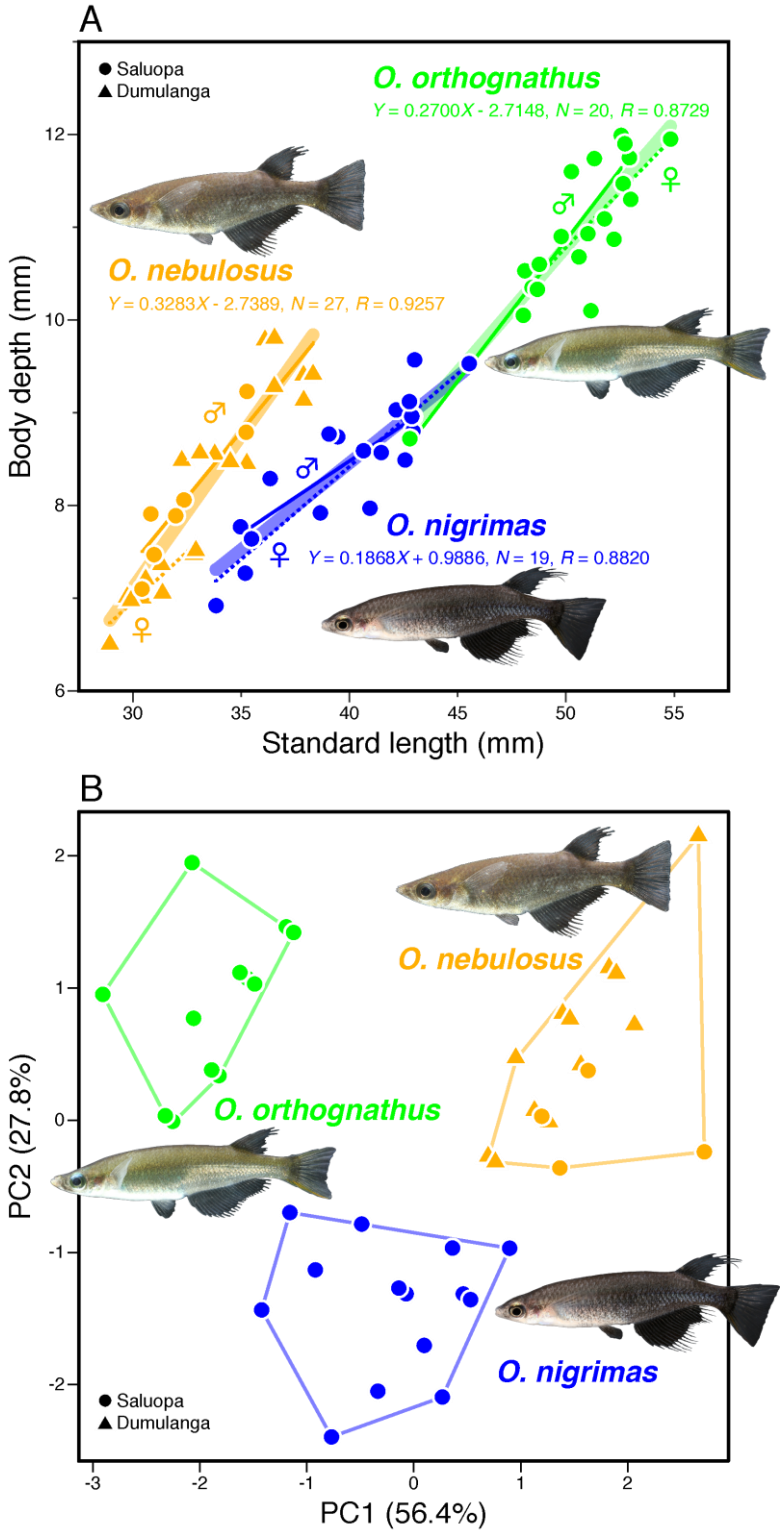

Figure 6. (A) Relationships between the standard length and body depth of the three sympatric *Oryzias* species. (B) Scatterplot of the first two axes of the principal component analysis based on the meristic characters. Circles and triangles represent fish collected from Lake Poso at Saluopa and Dumulanga, respectively.

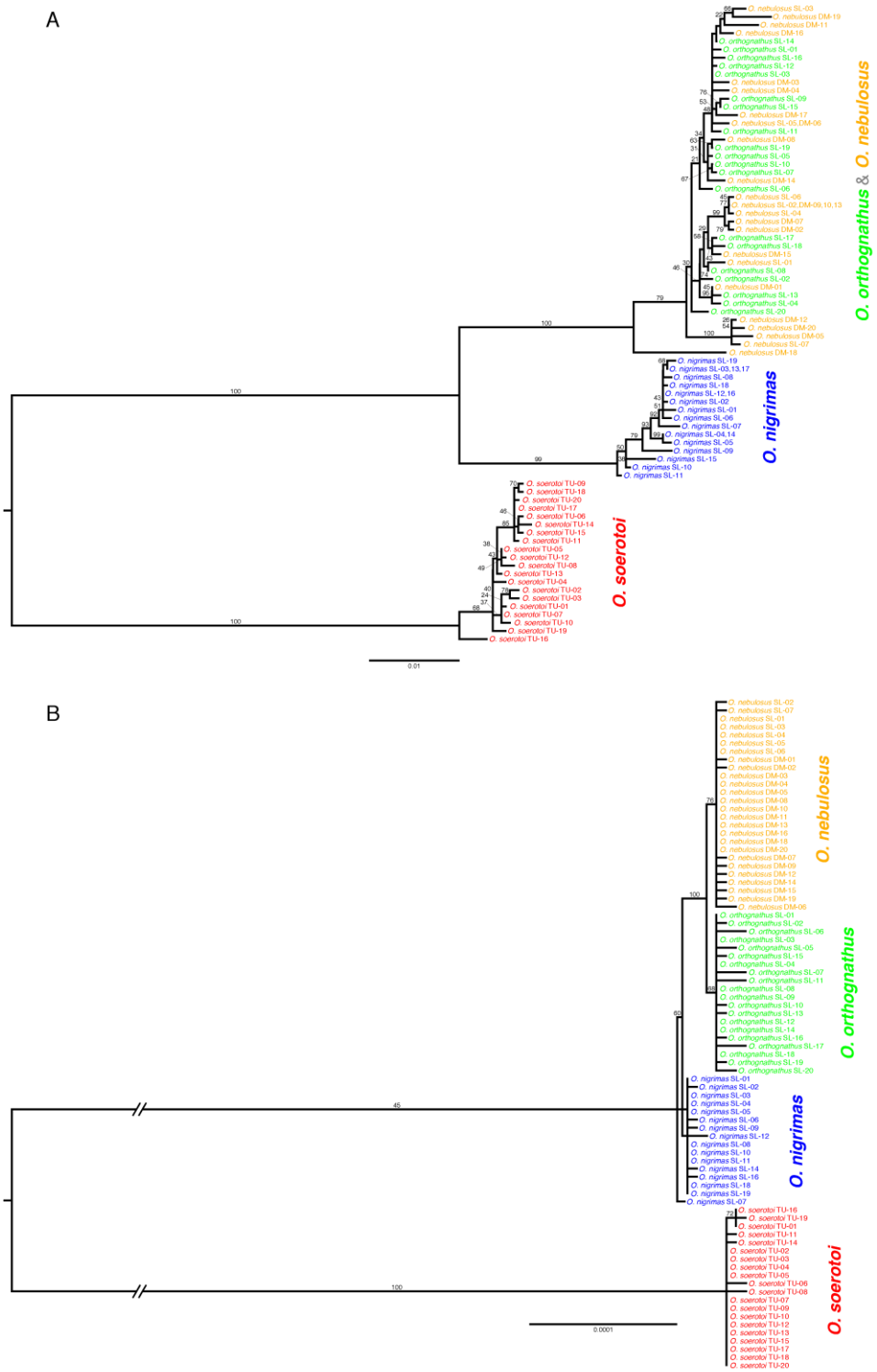

Figure 7. Maximum-likelihood and neighbor-joinging phylogenies of the three Poso *Oryzias* species with their outgroup, based on (A) the 2,194-bp concatenated mitochondrial sequences and (B) the 157,029-bp concatenated RAD sequences, respectively. Numbers on branches are bootstrap values.

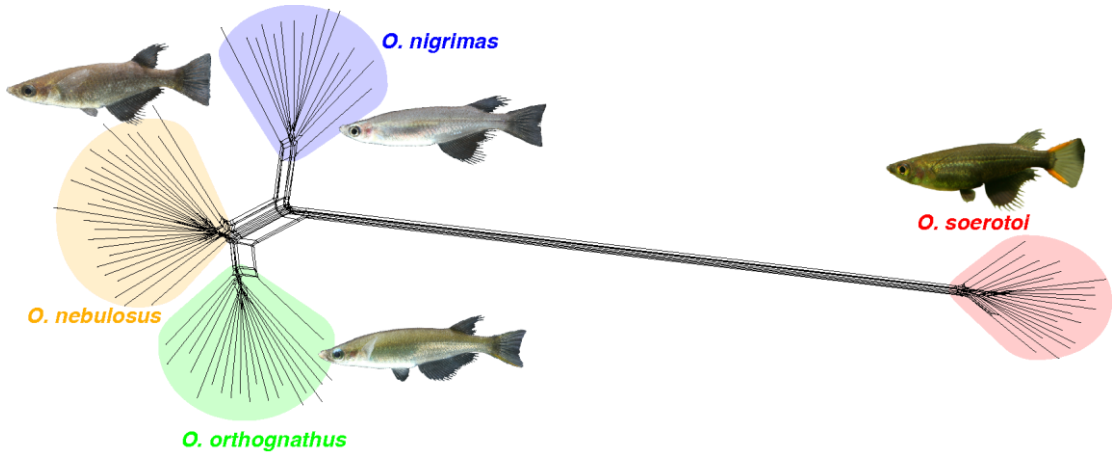

Figure 8. Neighbor-net phylogenetic networks based on Nei's genetic distances calculated from the 2,718 SNPs. Circles and triangles represent individuals collected from Saluopa and Dumulanga, respectively.

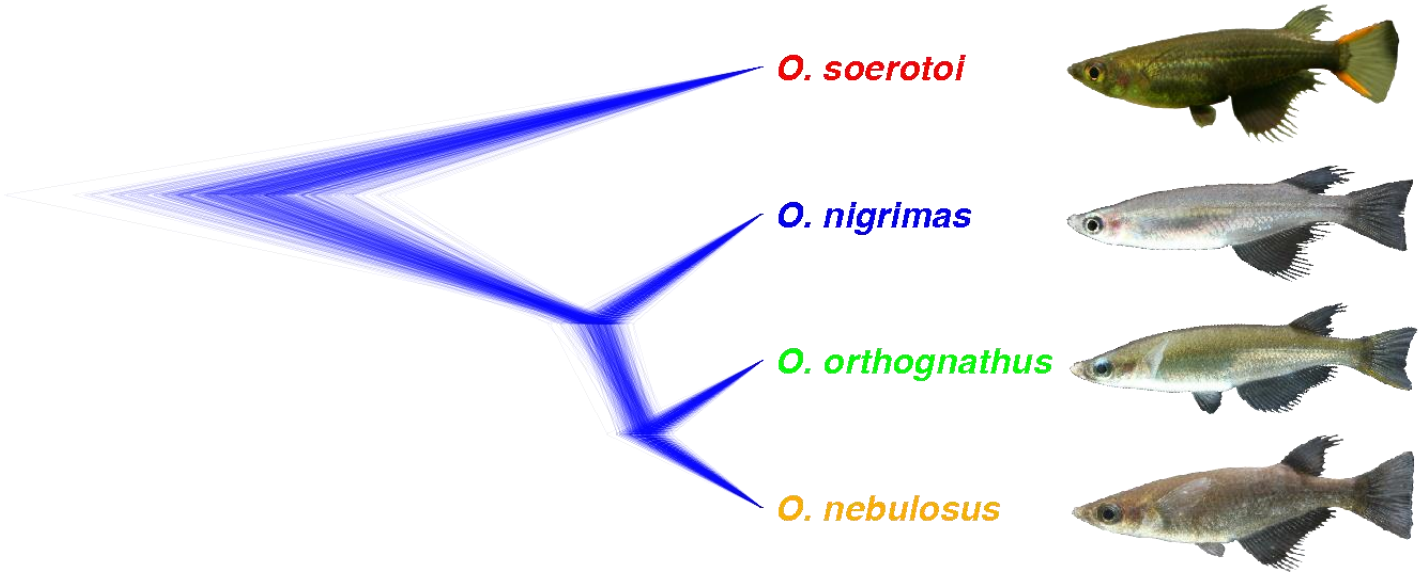

Figure 9. Species tree for the four *Oryzias* species estimated by SNAPP, based on 2,718 SNPs. Thin lines represent individual speciation trees.

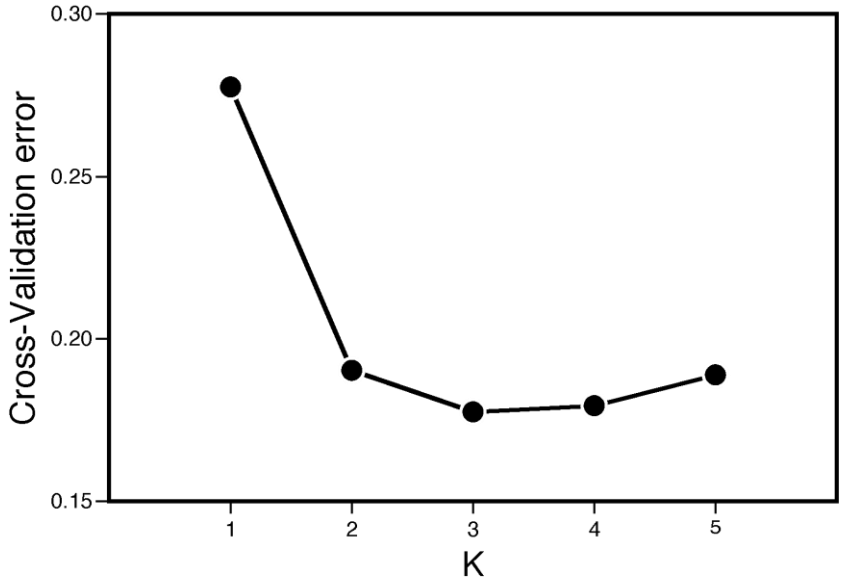

Figure 10. Cross-validation errors for the ADMIXTURE runs.

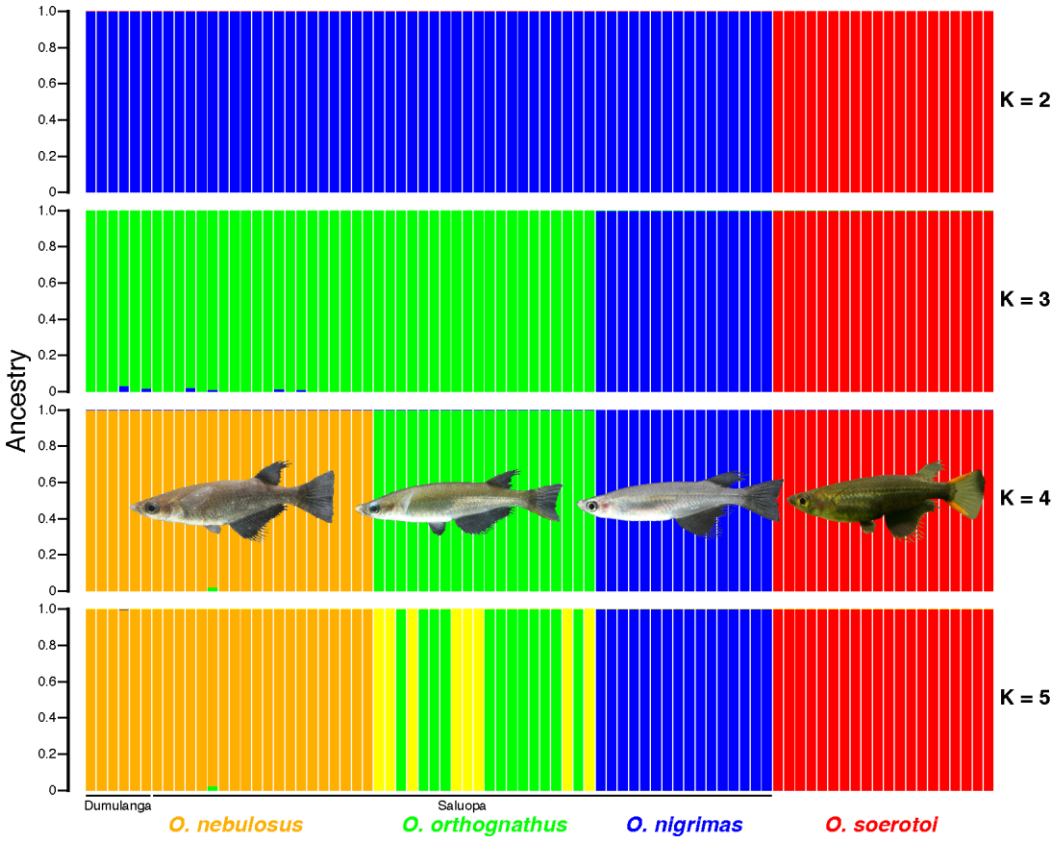

Figure 11. Results of ADMIXTURE analyses showing K = 2–5 genetic clusters, based on the2,718 SNPs.

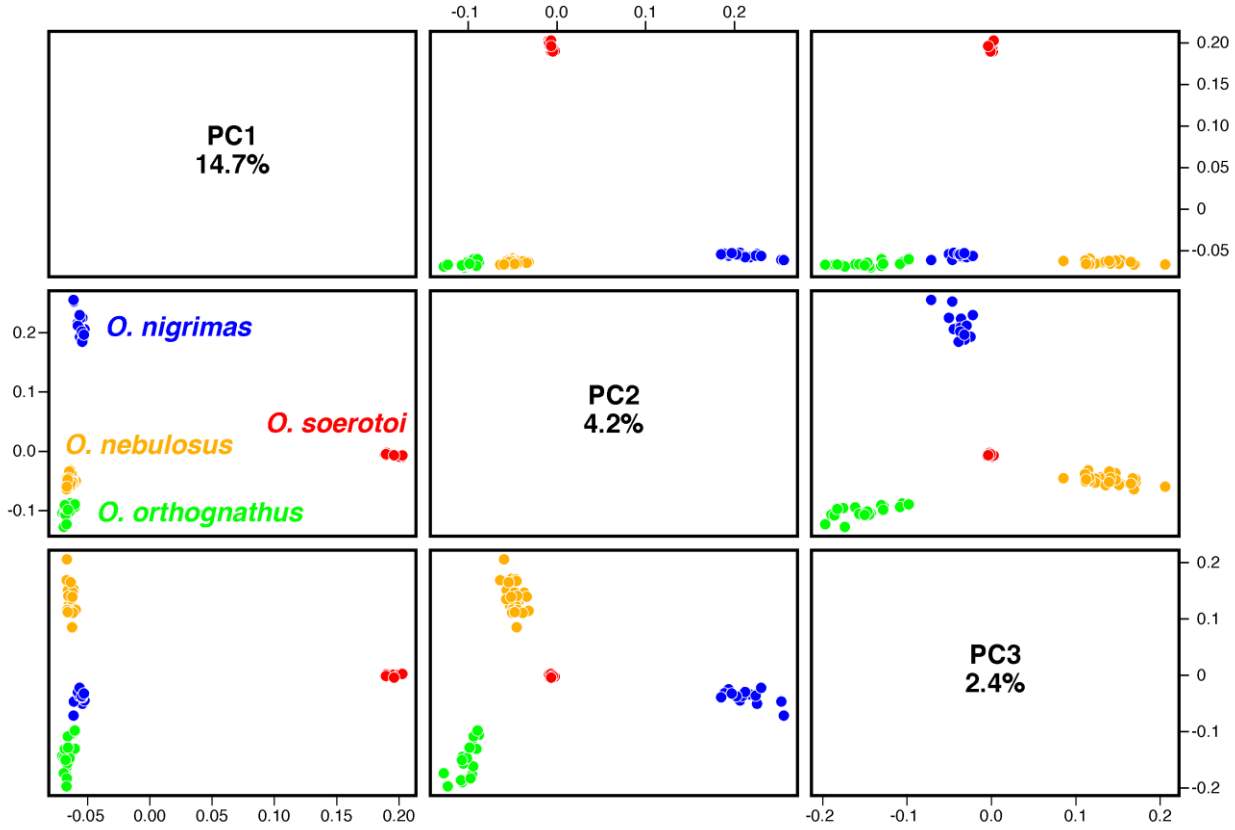

Figure 12. Principal components analysis of genetic variance among the four *Oryzias* species based on the 2,718 SNP dataset.

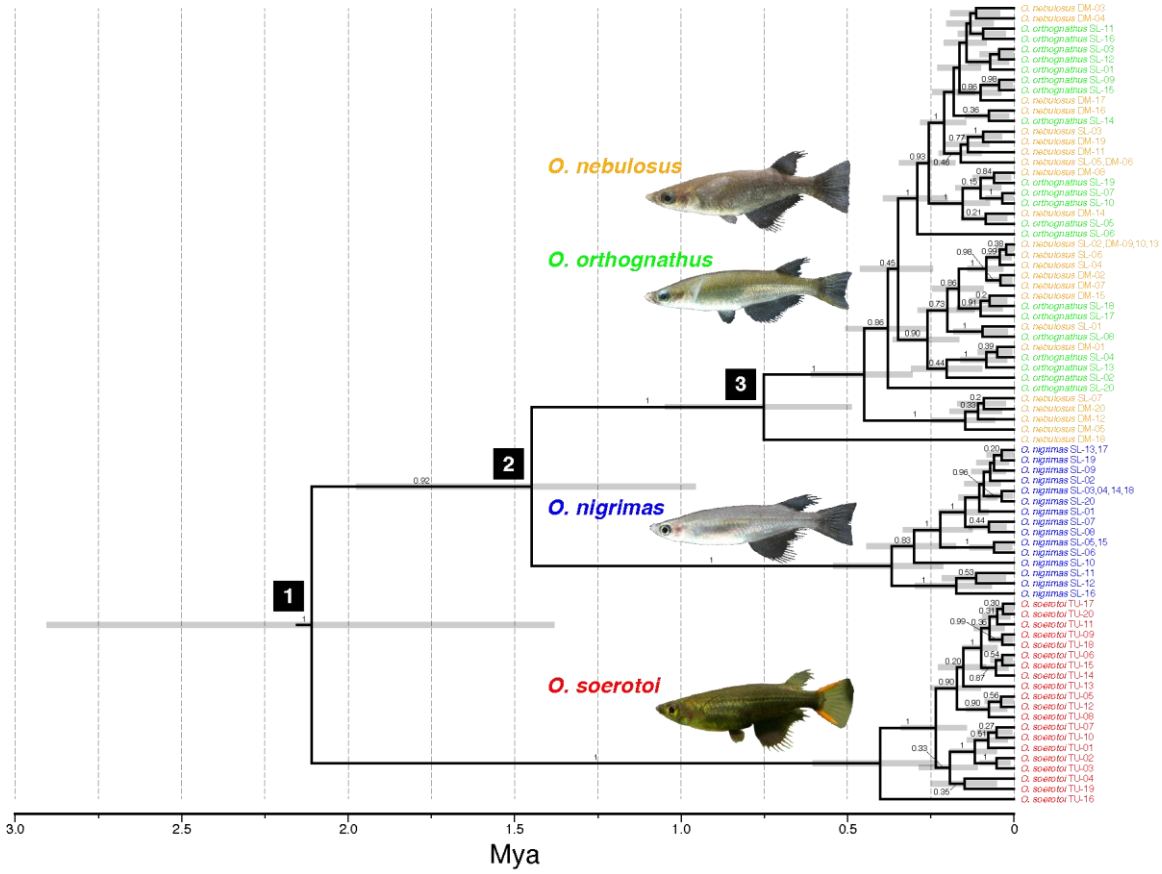

Figure 13. Bayesian chronogram based on the mtDNA sequences (ND2: 1,053 bp; cyt *b*: 1,141 bp), using substitution rates of 2.80% and 2.65% per Myr for ND2 and cyt *b*, respectively. Numbers on branches are Bayesian posterior probabilities. Bars represent 95% high posterior density.

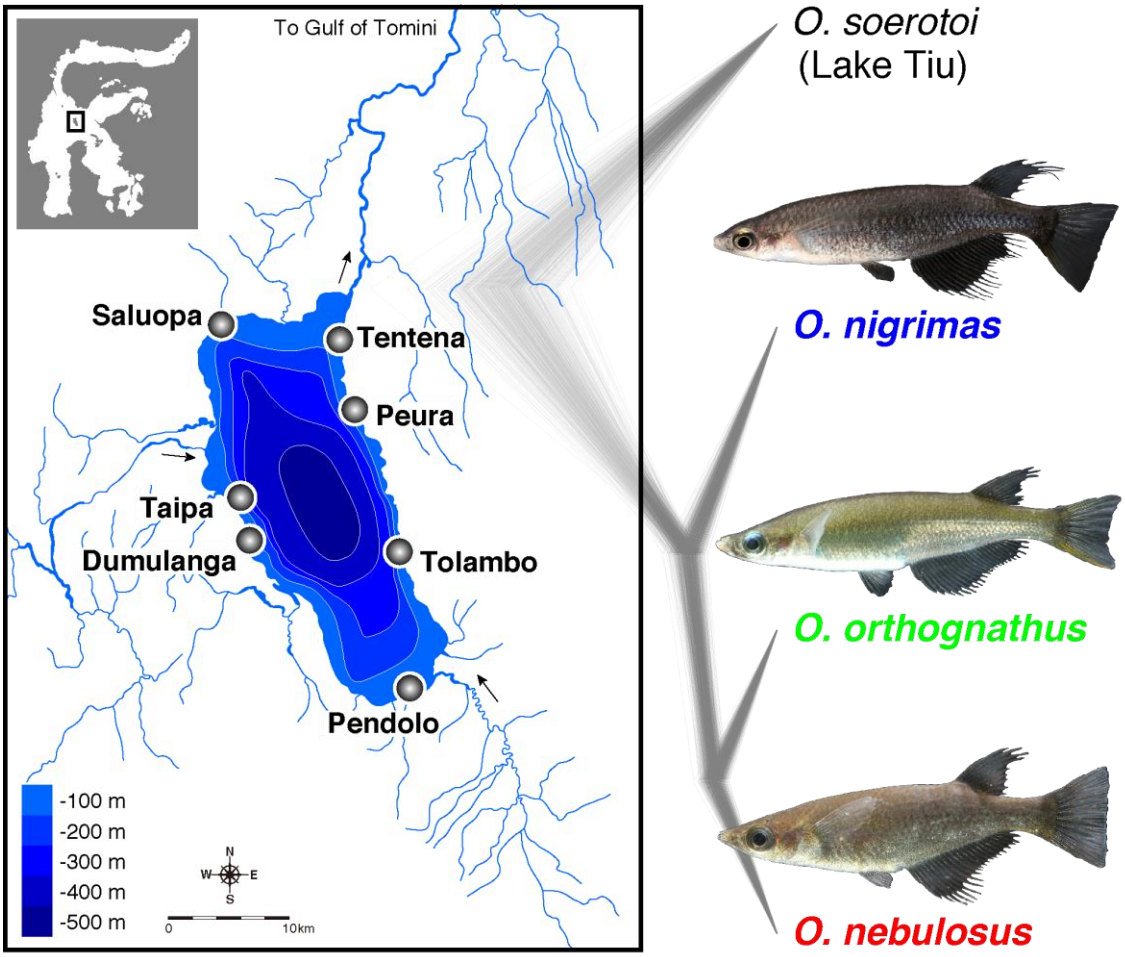

Figure 14. A map showing locations of the collection sites and species trees of three *Oryzias* species in Lake Poso. The map was provided by Thomas von Rintelen and modified.

Figure 15. Measurements of the gill raker lengths and intervals between adjacent gill rakers.

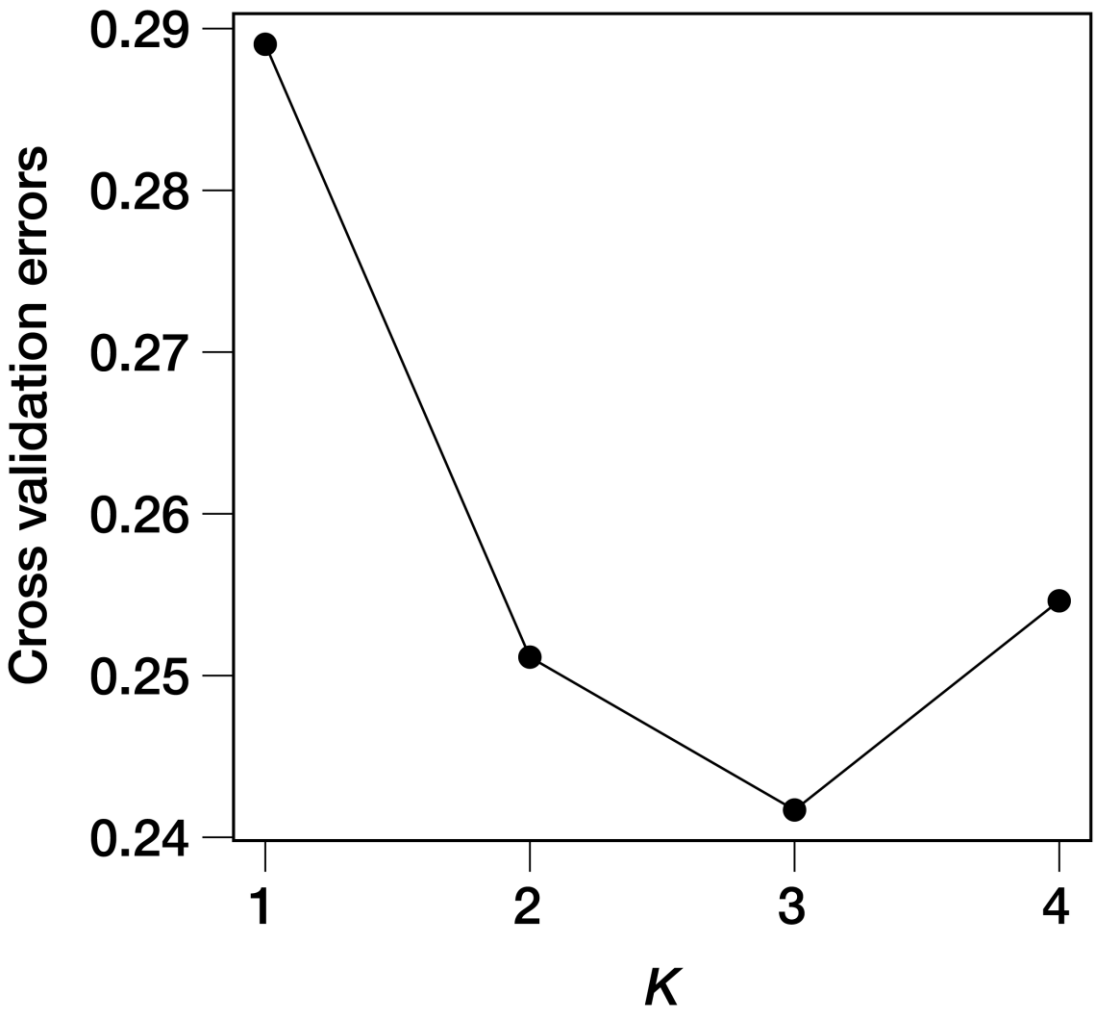

Figure 16. Cross-validation errors for the ADMIXTURE runs.

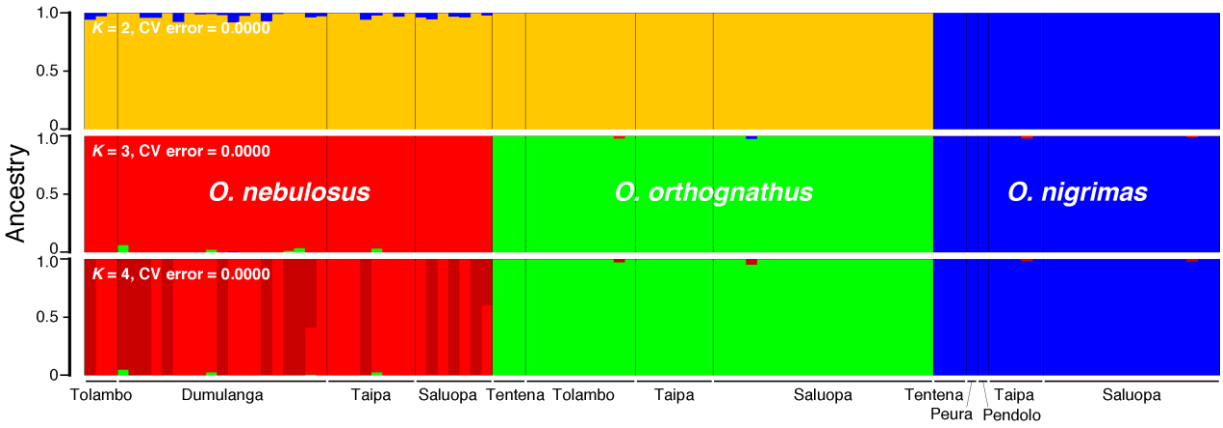

Figure 17. ADMIXTURE results showing *K* = 2–4 genetic clusters based on the 0,000 SNPs among four populations

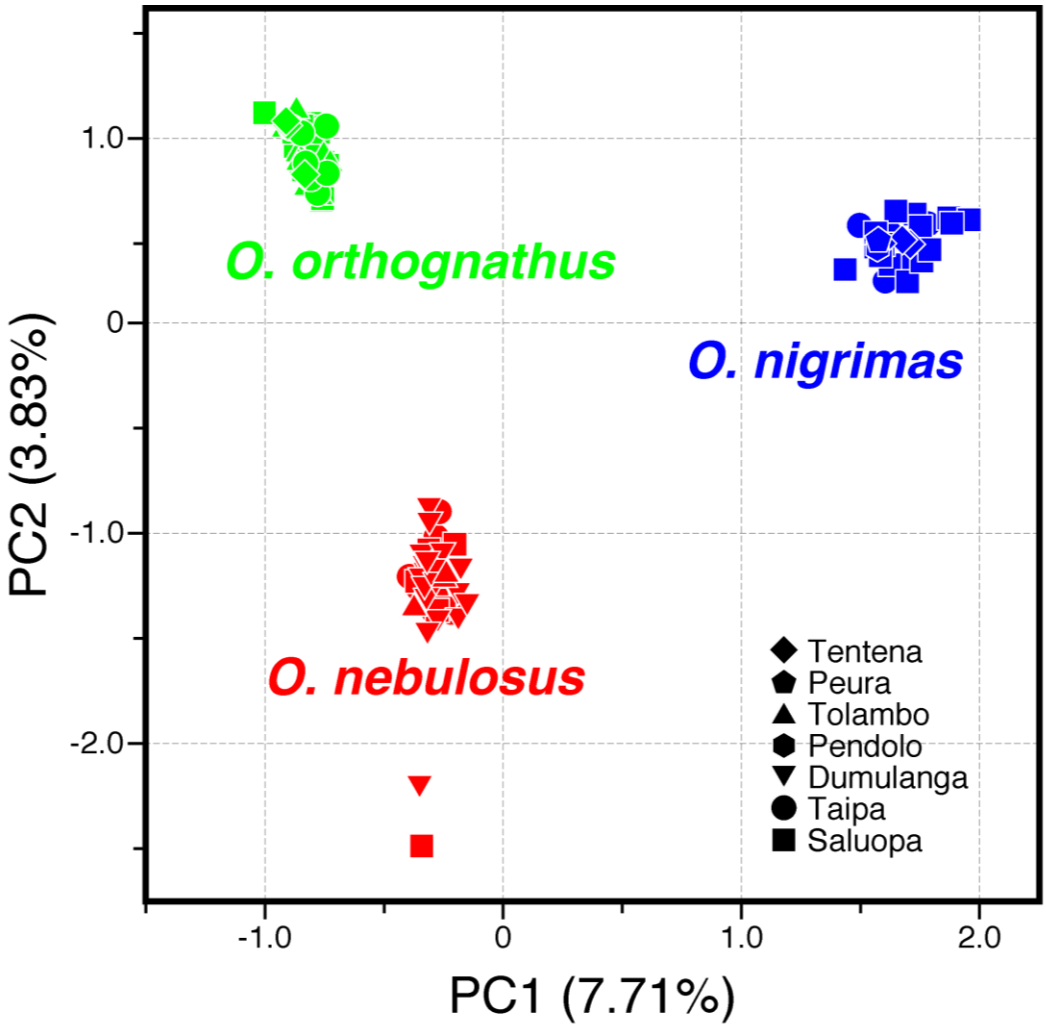

Figure 18. Principle component analysis of genetic variance among the three *Oryzias* species based on the 1,879 SNP dataset.

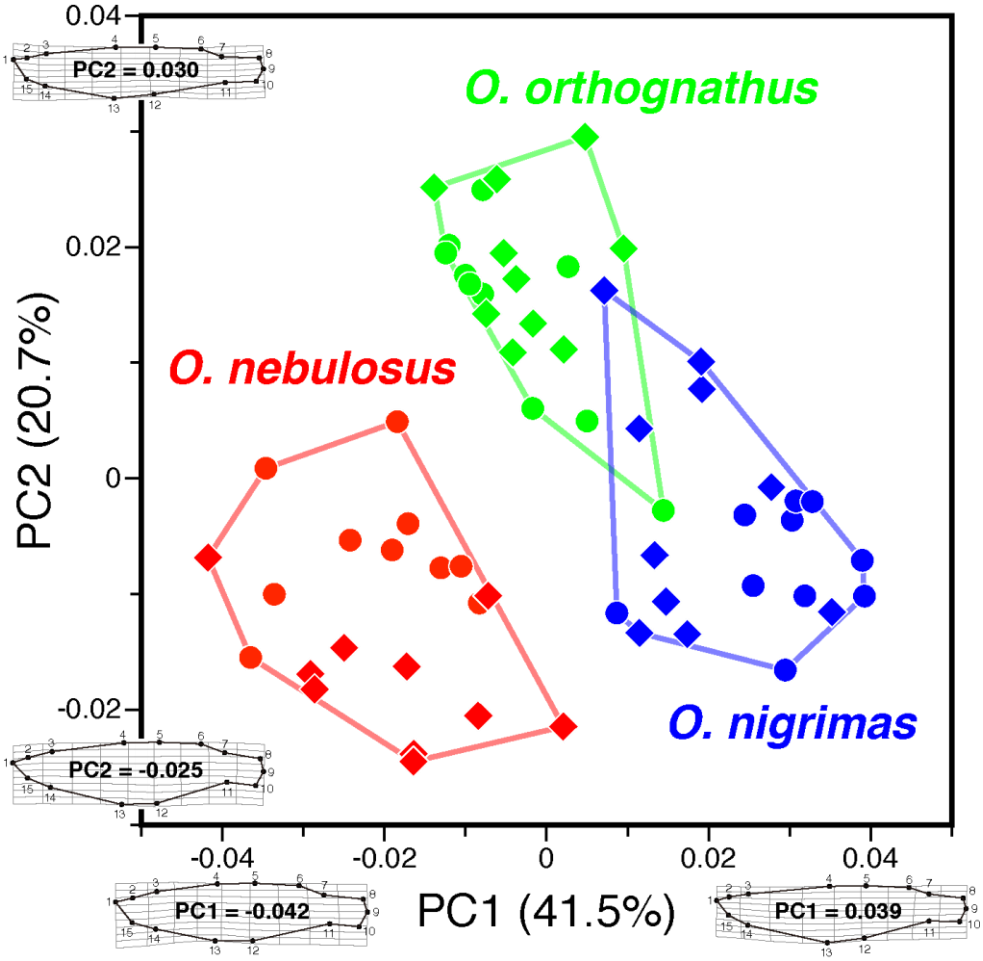

Figure 19. Scatterplot of the first two axes of principal component analyses based on the geometric morphometric dataset and deformation grids showing the maximum shape changes along each axis. Diamonds and circles represent males and females, respectively.

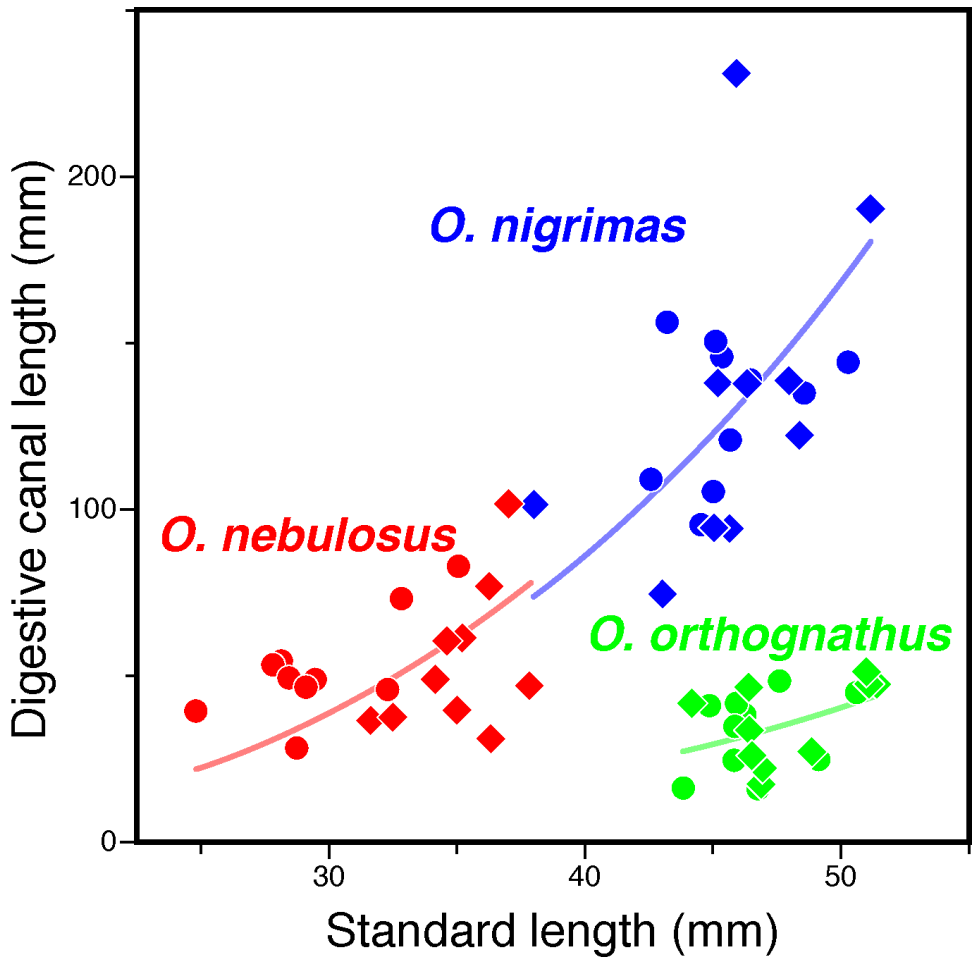

Figure 20. Relationship between the standard length and digestive tract length of the three *Oryzias* species. Diamonds and circles represent males and females, respectively.

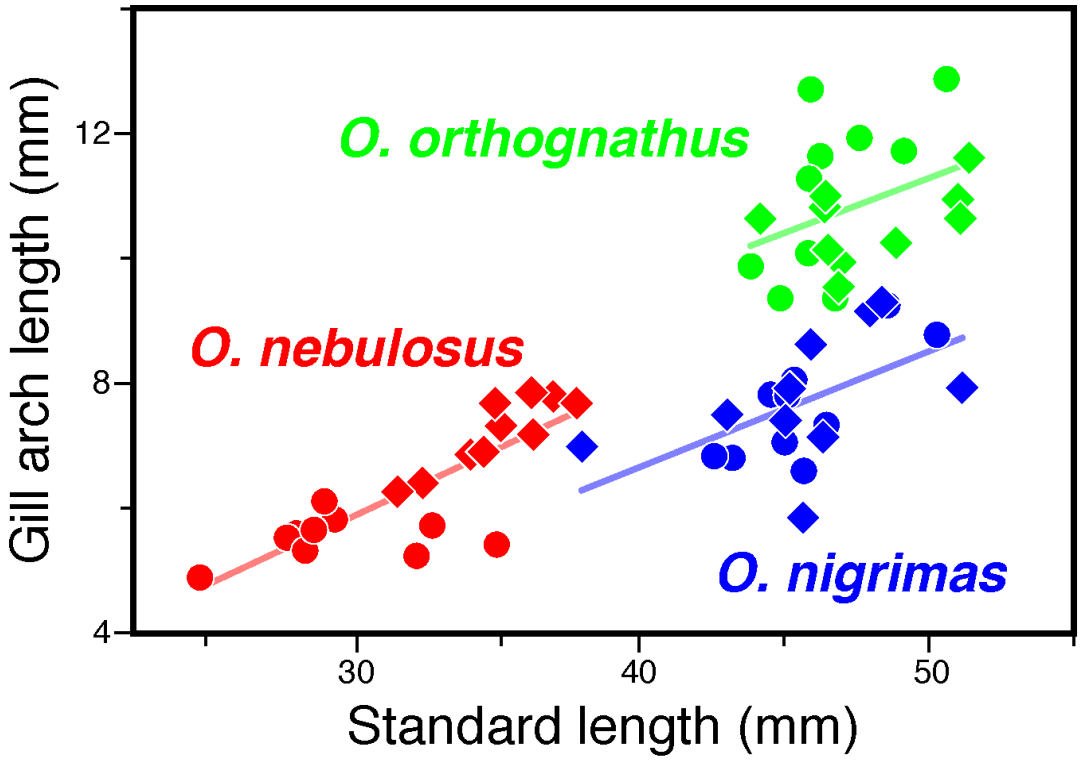

Figure 21. Relationship between the standard length and gill arch length of the three *Oryzias* species. Diamonds and circles represent males and females, respectively. The interspecific difference in gill arch length was significant after correcting the body size (ANCOVA, $F_{2,59}$ = 60.9493, $P < 0.0001$). The difference was significant (Turkey's HSD tests, $P < 0.05$) in all species pairs.

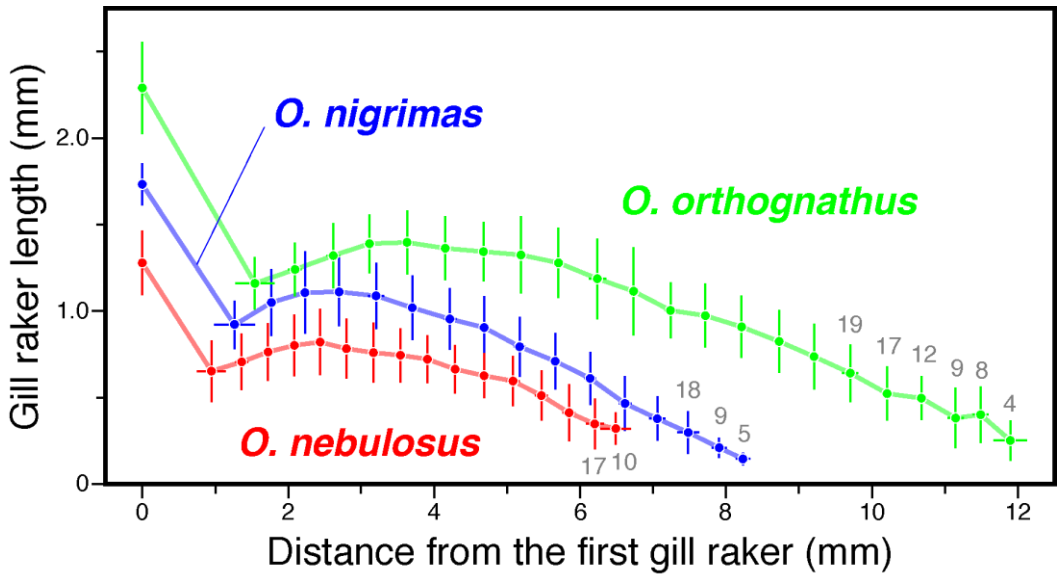

Figure 22. Length and distribution of each gill raker of the three *Oryzias* species.

Figure 23. Pictures of fresh digestive tracts of the three *Oryzias* species.

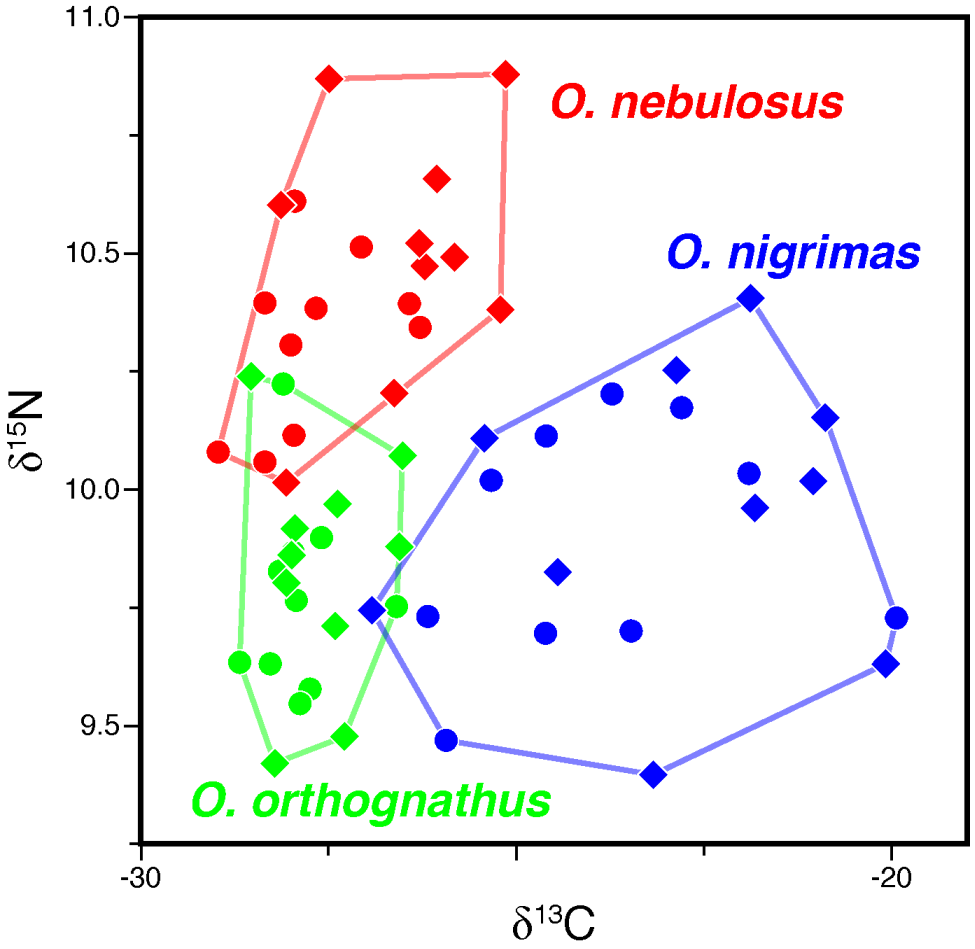

Figure 24. Plots of $\delta^{13}C$ versus $\delta^{15}N$ values of the three *Oryzias* species. Diamonds and circles represent males and females, respectively.

Figure 25. The spawning site of *Oryzias nebulosus* and *O. orthognathus* at Dumulanga. Darker and paler individuals are *O. nebulosus* and *O. orthognathus*, respectively.

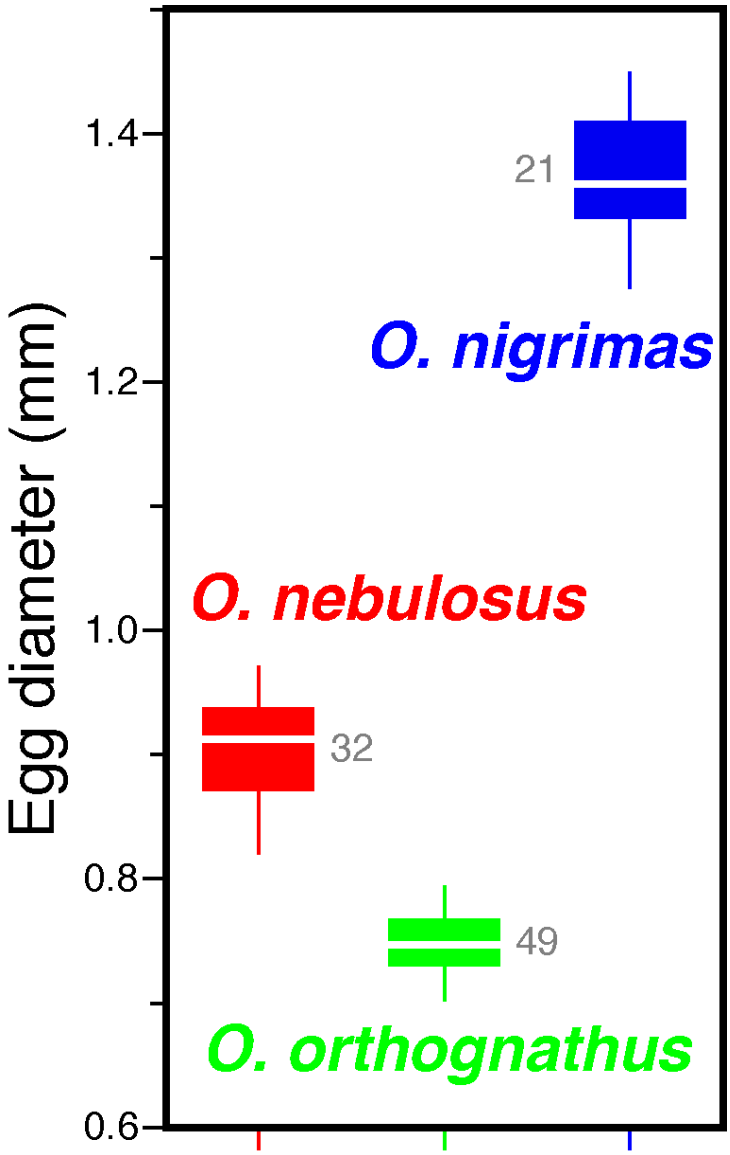

Figure 26. Egg diameters of the three *Oryzias* species. The line, box and whisker represent median, (upper and lower) quartiles, and range, respectively.

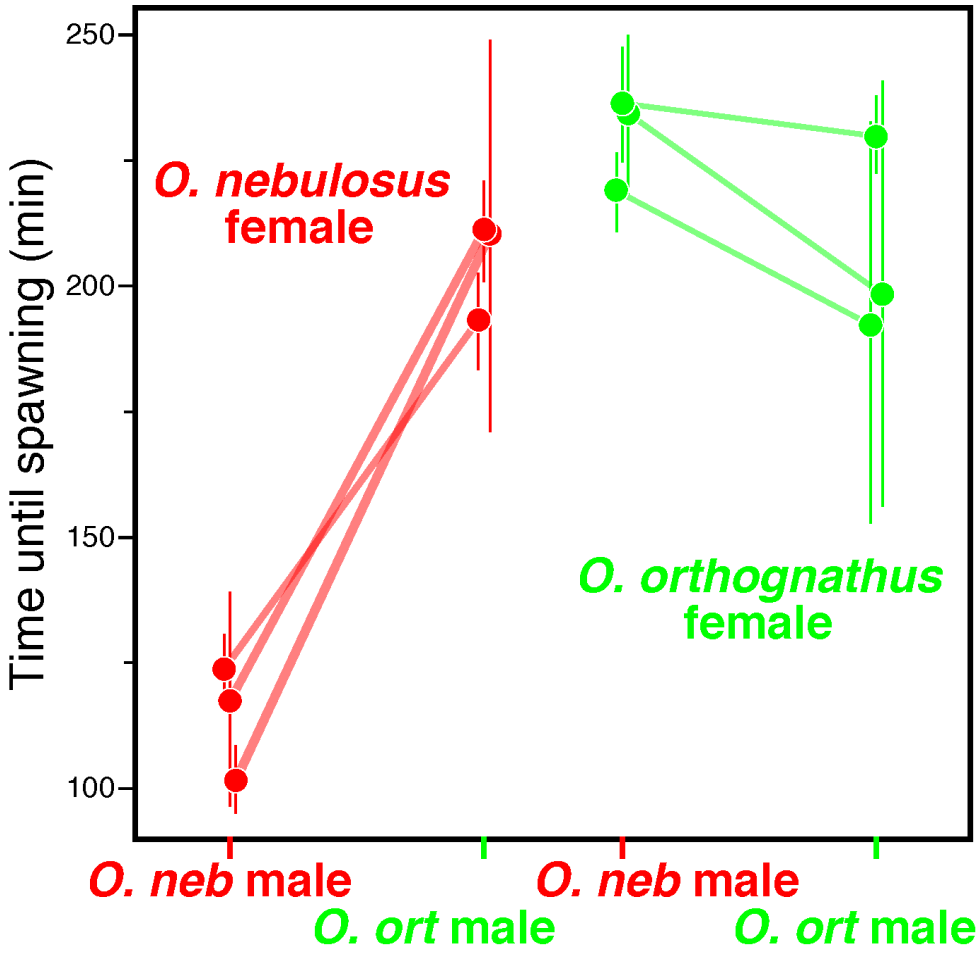

Figure 27. Time until spawning by each female of *Oryzias nebulosus* and *O. orthognathus*. Each line represents the average time (± SD) of one individual female mated with a male from the same versus different species.

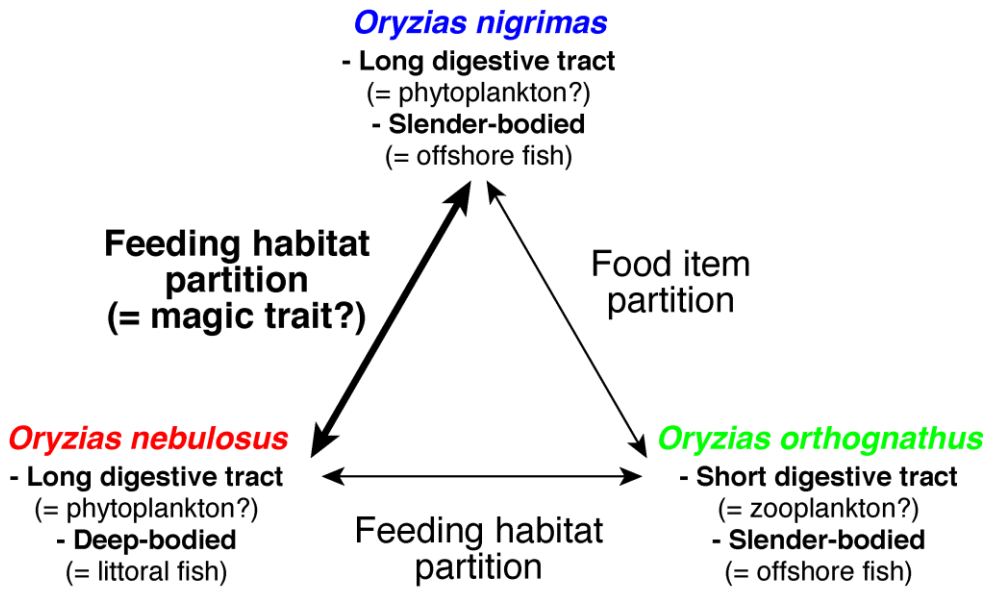

(B) Assortative mating

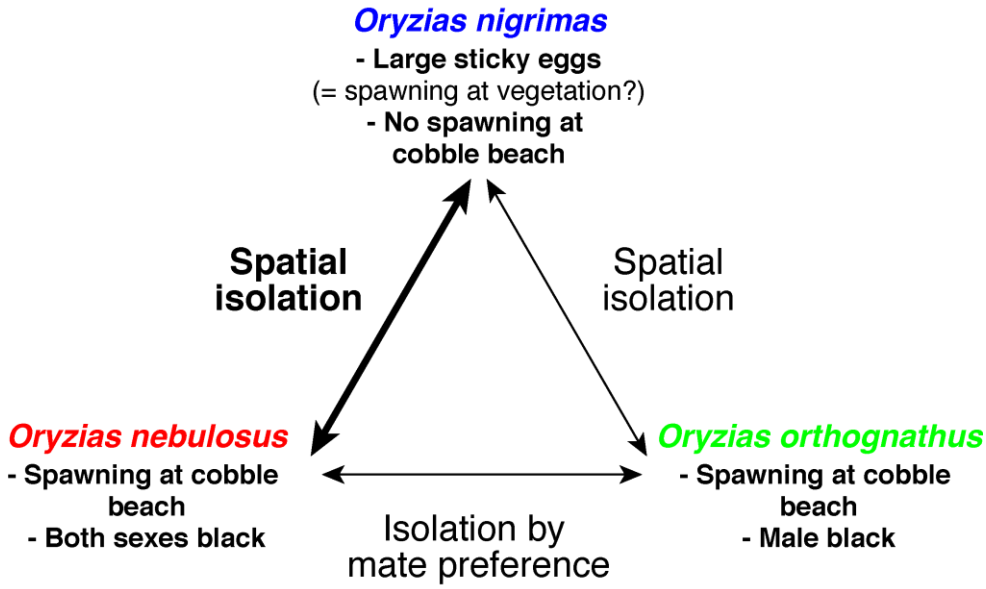

Figure 28. Summary of (A) resource partitioning and (B) assortative mating among the three Poso *Oryzias* species. Note that the difference in feeding sites between *O. nigrimas* and *O. nebulosus* may be an "automatic magic trait" leading to a “mate-where-you-eat” preference. However, no such automatic magic trait is evident between *O. nigrimas* and *O. orthognathus* or between *O. nebulosus*, and *O. orthognathus*.

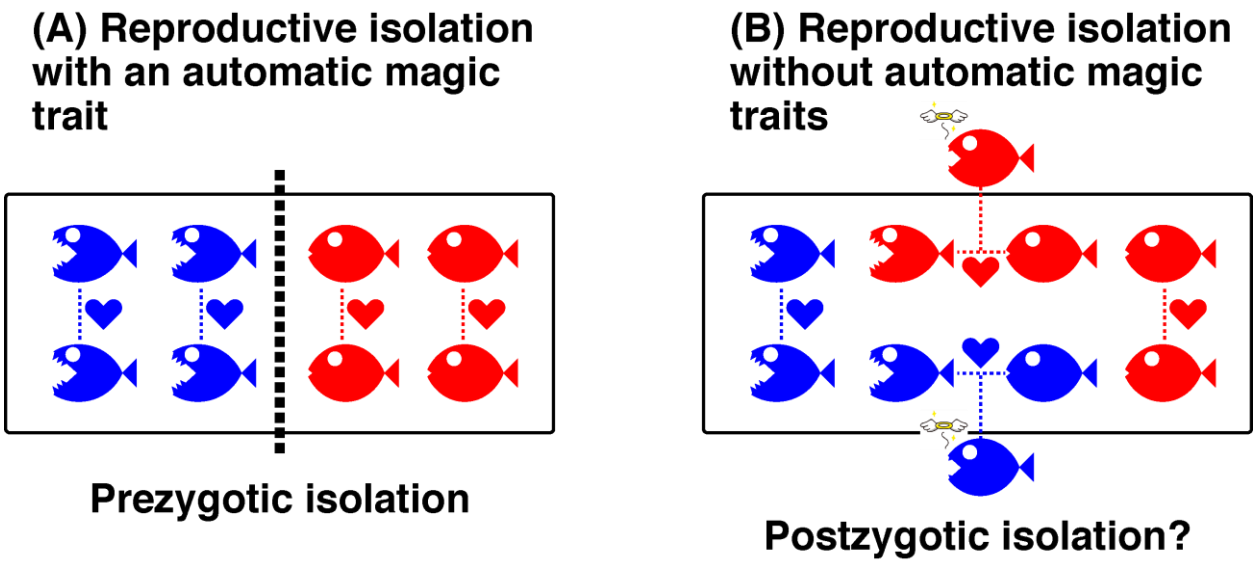

Figure 29. Schematic illustration to explain how sympatric speciation can be completed even without automatic magic traits. (A) Sympatric speciation with an automatic magic trait; sympatric speciation is considered to be completed, if resource partitioning and assortative mating are automatically coupled with each other. In contrast, (B) sympatric speciation would be possible even without such automatic magic traits, if there is a strong postzygotic isolation between diverging populations. The low-productivity ecosystem in Lake Poso would generate this situation, because hybrid individuals might not exploit the food resources.